



Research article

Bayesian estimation and prediction of Weibull current records with application to Saudi industrial data

Ramy Abdelhamid Aldallal*

Department of Management, College of Business Administration Hawtat Bani Tamim, Prince Sattam bin Abdulaziz University, Saudi Arabia

* **Correspondence:** Email: r.eldallal@psau.edu.sa.

Abstract: In this paper, we investigated the estimation and prediction problems based on current record statistics arising from the Weibull distribution. The Weibull model is widely used in industrial reliability, survival analysis, and environmental sciences. Under the assumption that the data represent current records from a two-parameter Weibull distribution with shape parameter k and scale parameter λ , we derived the new probability density function (PDF) and cumulative distribution function (CDF) of upper and lower current records. After that, a closed-form expression for the moments of upper and lower current records was obtained. Later, the maximum likelihood and Bayesian estimators for the parameters were obtained, along with predictions of future current record values and a predictive interval. Monte Carlo simulation was performed to assess the performance of the proposed estimators under various sample sizes and parameter settings. The methodology was further illustrated using an application to industrial data from Saudi Arabia, demonstrating the practical relevance of Weibull record modeling for reliability and life-testing analysis.

Keywords: Weibull distribution; current records; maximum likelihood and Bayesian estimation; prediction; Saudi Arabian industry data

Mathematics Subject Classification: 62E10, 62R01

1. Introduction

Record values naturally arise in various fields, including industrial reliability testing, climate studies, sports statistics, and finance. A record value occurs when an observation exceeds (upper record) or falls below (lower record) all previous observations. In many real-world settings, only the most recent record, or a sequence of the most recent records, may be observed; these are termed current records.

Record statistics constitute a well-established branch of order statistics concerned with observations

that exceed or fall below all previous values in a sequence of independent and identically distributed random variables. Classical results describe the probabilistic structure, inter-arrival times, and distributions of record values and record times, many of which possess distribution-free properties. These characteristics make record statistics particularly useful when full samples are unavailable or when only extreme observations are retained. Current records extend this framework by focusing on the most recent record information available at each stage, rather than the entire record sequence, thereby providing a more realistic representation for practical situations where only the latest record observations are stored or monitored.

The Weibull distribution is a flexible lifetime model that generalizes the exponential and Rayleigh distributions. Its versatility makes it a popular choice in reliability and failure-time studies. When data are available as record observations rather than complete samples, estimation and prediction require special treatment because the likelihood function is derived from record-specific distributions.

Predicting future current record values plays a crucial role in many statistical, engineering, and scientific applications. Current records, whether upper, lower, or based on their ranges, capture the most extreme observations within a sequential dataset and therefore reflect critical structural changes in underlying processes. Forecasting future record values provides valuable insight into the expected behavior of extremes, improves risk assessment, and enhances decision-making across fields such as reliability testing, climate studies, finance, and environmental monitoring. Moreover, accurate prediction of future current records enables practitioners to anticipate potential failures, extreme events, or performance limits before they occur.

In this study, we develop a comprehensive inferential framework for current-record data modeled by the two-parameter Weibull distribution. We present classical and Bayesian estimation procedures, derive predictive intervals, and apply the methodology to industrial data from Saudi Arabia. The research is particularly relevant to the Kingdom of Saudi Arabia's prioritized industrial development under its Vision 2030 framework, which places "leadership in energy and industry" among its key national goals. Accurate prediction of current record-based performance directly supports this strategic objective by enhancing the reliability, efficiency, and longevity of critical industrial and energy infrastructure, thereby contributing to economic diversification and technological advancement.

This work builds upon a substantial body of research on current records. Aldallal [8] examined current record ranges for Laplace-distributed Saudi industrial data, extending earlier foundational work. Additionally, in [9], for the Rayleigh current records, he estimated the distribution's parameters and constructed prediction intervals for future record values. Barakat et al. [11] established key results for moments and recurrence relations of current records under various distributions, while Aldallal [7] derived similar properties for the Generalized Exponential distribution. Raqab [19, 21] developed bounds for expectations of record ranges and increments, and Ahmadi and Balakrishnan [5] later used current records to construct prediction intervals for order statistics; an approach by Chahkandi and Ahmadi [13] extended to (k) -records.

The development of distribution-free prediction intervals for future records has been another active area, addressed by Barakat et al. [12], Raqab [20], and Ahmadi and Balakrishnan [2]. Related contributions include Aldallal's [6] work on Kumaraswamy-distributed records and Ahmadi et al.'s [4] introduction of generalized "Current (k) -records". Furthermore, Ahmadi and Balakrishnan [1, 3] studied the current record range for constructing quantile confidence intervals and investigating its reliability properties.

In this paper, we adopt the following notation for a sequence $\{X_m\}$: Let LC_m and UC_m denote the lower and upper current records, respectively, observed at the m th record event. By definition, $LC_{m+1} = LC_m$ when a new upper record occurs ($UC_{m+1} > UC_m$), and $UC_{m+1} = UC_m$ when a new lower record occurs ($LC_{m+1} < LC_m$). Thus, LC_m represents the minimum observation up to the m th record point, with initial values $UC_0 = LC_0 = X_1$. For $m \geq 1$, the interval (LC_m, UC_m) is termed the record coverage, and the current record range is defined as $RC_m = UC_m - LC_m$. A new range is recorded each time either a new upper or lower current record is established.

In Section 2, we derive the cumulative distribution function (CDF) and probability density function (PDF) for upper and lower current records when the underlying data follow a two-parameter Weibull distribution. In Section 3, we present closed-form expressions for the moments of these records, facilitating analysis of their central tendency and variability. Parameter estimation, including maximum likelihood and Bayesian approaches for upper and lower current records, is detailed in Section 4. In Section 5, we introduce the prediction of future upper current records, lower current records, and record ranges, along with the construction of corresponding prediction intervals using two approaches. Finally, Section 6 is divided into two parts: A simulation study to evaluate the performance of the proposed estimators and predictors, and a real-data analysis using Saudi Arabian industrial data to demonstrate the practical utility of the methodology.

2. PDF and CDF of Weibull current record distributed data

Finding the CDF and PDF for some data is crucial because they provide a full probabilistic description of how the data is distributed, which is essential for parameter estimation, prediction, and risk analysis [17, 18]. In this section, we derive the CDF and PDF of the current lower (upper) record when the original data follow a Weibull distribution.

The PDF and CDF of the Weibull distribution with scale parameter $\lambda > 0$ and shape parameter $k > 0$ are given, respectively, by:

$$f(x; k, \lambda) = \frac{k}{\lambda} \left(\frac{x}{\lambda}\right)^{k-1} e^{-\left(\frac{x}{\lambda}\right)^k}, \quad x \geq 0, \quad (2.1)$$

$$F(x; k, \lambda) = 1 - e^{-\left(\frac{x}{\lambda}\right)^k}. \quad (2.2)$$

Parameter λ stretches or compresses the distribution along the horizontal axis. Statistically, it controls the scale or typical size of observations. Larger values of λ mean the observations tend to be larger and vice versa. Moreover, the parameter k controls the shape of the Weibull distribution:

- For $k < 1$, the distribution has a heavy right tail (useful for modeling early-failure data).
- For $k = 1$, it reduces to the exponential distribution.
- For $k = 2$, it reduces to the Rayleigh distribution.
- For $k \geq 3$, the distribution becomes increasingly symmetric and concentrated near its mean.

Theorem 1. For $m > 1$, the CDF and PDF of the lower (upper) current records, when the original data follows a Weibull distribution, are, respectively, given by:

$$F_{LC_m}(x; k, \lambda) = 1 + 2^m \left(1 - e^{-\left(\frac{x}{\lambda}\right)^k}\right) P\left(m, -\log\left(1 - e^{-\left(\frac{x}{\lambda}\right)^k}\right)\right)$$

$$- P\left(m, -2 \log(1 - e^{-(x/\lambda)^k})\right), \quad (2.3)$$

$$f_{LC_m}(x; k, \lambda) = 2^m \frac{k}{\lambda} \left(\frac{x}{\lambda}\right)^{k-1} e^{-(x/\lambda)^k} P\left(m, -\log(1 - e^{-(x/\lambda)^k})\right), \quad (2.4)$$

$$F_{UC_m}(x; k, \lambda) = P\left(m, \left(\frac{x}{\lambda}\right)^k\right) - 2^m e^{-(x/\lambda)^k} P\left(m, \frac{1}{2} \left(\frac{x}{\lambda}\right)^k\right), \quad (2.5)$$

$$f_{UC_m}(x; k, \lambda) = \frac{2^m k}{\lambda} \left(\frac{x}{\lambda}\right)^{k-1} e^{-(x/\lambda)^k} P\left(m, \frac{1}{2} \left(\frac{x}{\lambda}\right)^k\right), \quad (2.6)$$

where $P(a, b)$ is the regularized lower Gamma function.

Proof. To find the CDF and PDF of the current record when the data follows a Weibull distribution, we start from the general Houchens formulas [15]:

$$F_{LC_m}(x) = 2^m F(x) \left\{ 1 - F(x) \sum_{k=0}^{m-1} 2^{-(k+1)} \sum_{j=0}^k \frac{[-2 \log F(x)]^j}{j!} \right\}, \quad (2.7)$$

$$f_{LC_m}(x) = 2^m f(x) \left\{ 1 - F(x) \sum_{k=0}^{m-1} \frac{[-\log F(x)]^k}{k!} \right\}, \quad (2.8)$$

$$F_{UC_m}(x) = 1 - 2^m \bar{F}(x) \left\{ 1 - \bar{F}(x) \sum_{k=0}^{m-1} 2^{-(k+1)} \sum_{j=0}^k \frac{[-2 \log \bar{F}(x)]^j}{j!} \right\}, \quad (2.9)$$

$$f_{UC_m}(x) = 2^m f(x) \left\{ 1 - \bar{F}(x) \sum_{k=0}^{m-1} \frac{[-\log \bar{F}(x)]^k}{k!} \right\}, \quad (2.10)$$

where $\bar{F}(x) = 1 - F(x)$.

Substitute by (1) and (2) in (7), but after taking $t = (x/\lambda)^k$, we get:

$$F_{LC_m}(x) = 2^m (1 - e^{-t}) \left[1 - (1 - e^{-t}) \sum_{k=0}^{m-1} 2^{-(k+1)} \sum_{j=0}^k \frac{[-2 \log(1 - e^{-t})]^j}{j!} \right].$$

Define $u = -\log(1 - e^{-t})$, then the inner double sum becomes

$$S = \sum_{k=0}^{m-1} 2^{-(k+1)} \sum_{j=0}^k \frac{(2u)^j}{j!}.$$

Changing the order of summation gives

$$S = \sum_{j=0}^{m-1} \frac{(2u)^j}{j!} \sum_{k=j}^{m-1} 2^{-(k+1)} = \sum_{j=0}^{m-1} \frac{(2u)^j}{j!} 2^{-j} (1 - 2^{-(m-j)}) = \sum_{j=0}^{m-1} \frac{u^j}{j!} (1 - 2^{-(m-j)}).$$

Splitting the sum yields

$$S = \sum_{j=0}^{m-1} \frac{u^j}{j!} - 2^{-m} \sum_{j=0}^{m-1} \frac{(2u)^j}{j!}.$$

Using the identity $\sum_{r=0}^{m-1} \frac{z^r}{r!} = e^z \left(1 - \frac{\gamma(m, z)}{(m-1)!}\right)$, we obtain

$$S = e^u \left(1 - \frac{\gamma(m, u)}{(m-1)!}\right) - 2^{-m} e^{2u} \left(1 - \frac{\gamma(m, 2u)}{(m-1)!}\right).$$

Multiplying by $(1 - e^{-t})$ and using $e^u = 1/(1 - e^{-t})$ gives

$$(1 - e^{-t})S = 1 - \frac{\gamma(m, u)}{(m-1)!} - 2^{-m} e^u \left(1 - \frac{\gamma(m, 2u)}{(m-1)!}\right).$$

Substituting back into $F_{LC_m}(x)$ leads to

$$\begin{aligned} F_{LC_m}(x) &= 2^m(1 - e^{-t}) [1 - (1 - e^{-t})S] = 1 + 2^m(1 - e^{-t}) \frac{\gamma(m, u)}{m-1)!} - \frac{\gamma(m, 2u)}{(m-1)!} \\ &= 1 + 2^m(1 - e^{-t})P(m, u) - P(m, 2u), \end{aligned}$$

where $\gamma(m, z)$ is the incomplete Gamma function. Now, by re-substituting the values of t and u , one gets (3). To find (4), we use the same substitutions for t and u and perform a routine calculation to reach our goal.

For (5), and after substituting (1) and (2) in it, we get

$$F_{UC_m}(x) = 1 - 2^m e^{-t} \left\{ 1 - e^{-t} \sum_{k=0}^{m-1} 2^{-(k+1)} \sum_{j=0}^k \frac{[-2 \log e^{-t}]^j}{j!} \right\}.$$

Thus, the inner sum becomes $S = \sum_{k=0}^{m-1} 2^{-(k+1)} \sum_{j=0}^k \frac{(2t)^j}{j!}$. Additionally, by changing the order of summation, we can write $S = \sum_{j=0}^{m-1} \frac{t^j}{j!} - 2^{-m} \sum_{j=0}^{m-1} \frac{(2t)^j}{j!}$. Now, using the identity $\sum_{j=0}^{m-1} \frac{z^j}{j!} = e^z P(m, z)$, we reach $S = e^t P(m, t) - 2^{-m} e^{2t} P(m, 2t)$. Multiply by e^{-t} and simplify

$$e^{-t}S = e^{-t}(e^t P(m, t) - 2^{-m} e^{2t} P(m, 2t)) = P(m, t) - 2^{-m} e^t P(m, 2t).$$

Hence, the bracket simplifies to

$$1 - e^{-t}S = 1 - (P(m, t) - 2^{-m} e^t P(m, 2t)) = 1 - P(m, t) + 2^{-m} e^t P(m, 2t).$$

Multiplying by $2^m e^{-t}$ and simplifying gives

$$F_{UC_m}(x) = P(m, t) - 2^m e^{-t} P\left(m, \frac{t}{2}\right),$$

where the argument rescaling accounts for the factor $1/2$. By putting back the value of t , we reach (5). Moreover, (6) is a direct substitution of (1) and (2) in (10), and some easy steps, when you do it, you reach the proposed form. \square

Figures 1–4 are charts of the PDFs and CDFs of the lower (upper) current records in Theorem 1 for different values of m , k , and λ .

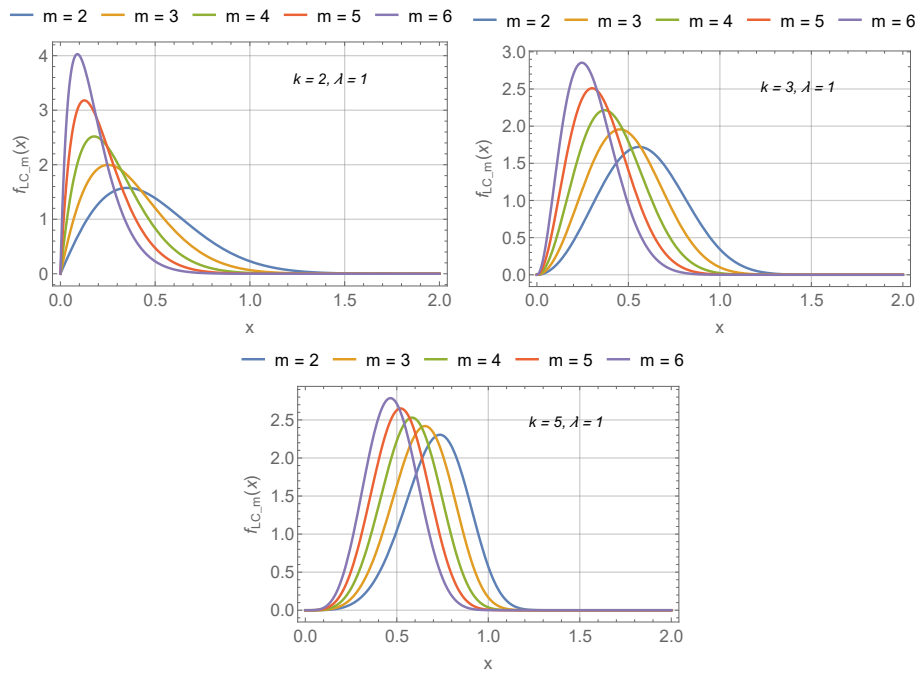


Figure 1. Plot of $f_{LC_m}(x)$ for different values of m, k , and λ .

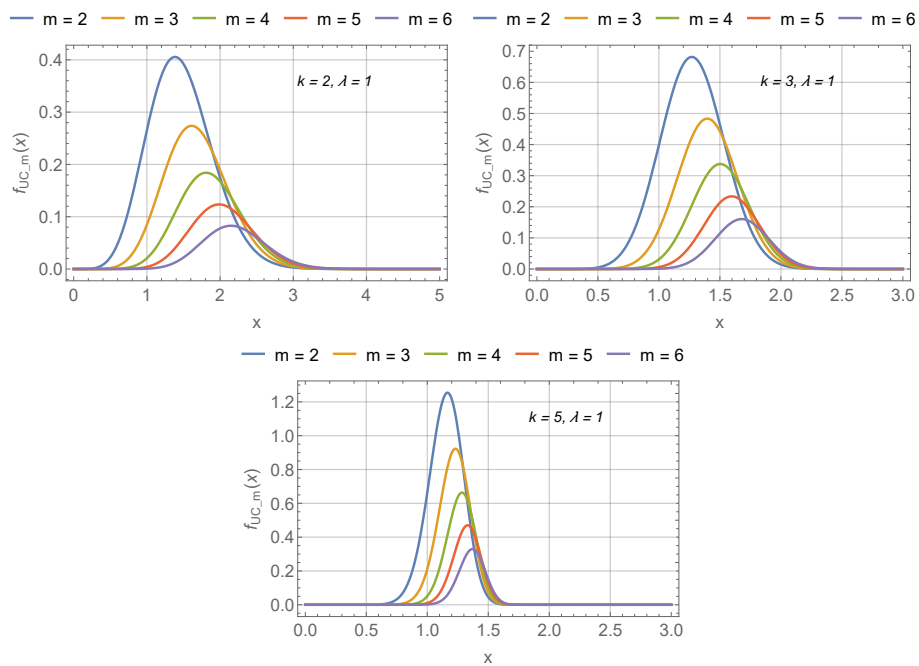


Figure 2. Plot of $f_{UC_m}(x)$ for different values of m, k , and λ .

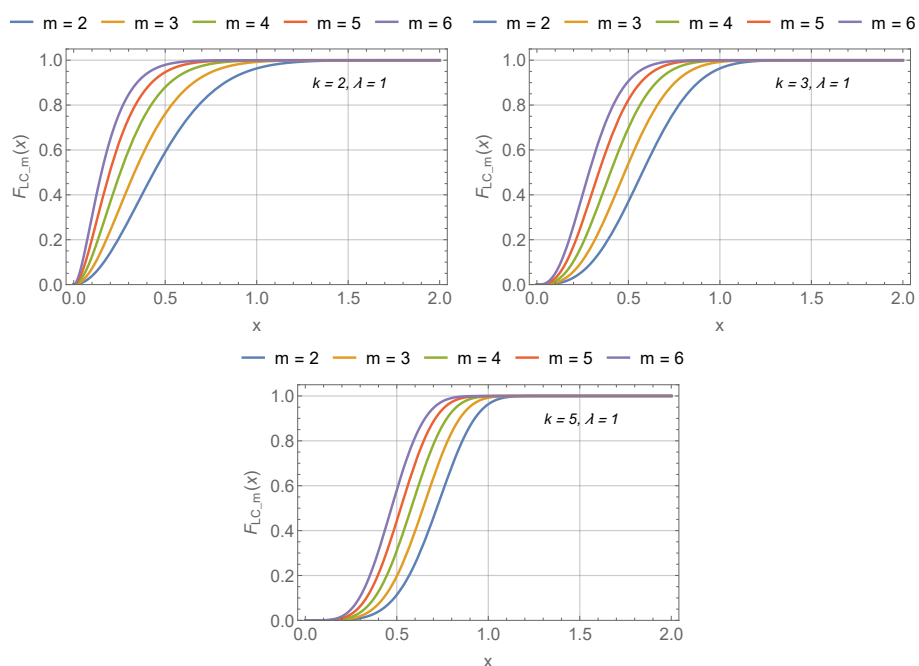


Figure 3. Plot of $F_{LC_m}(x)$ for different values of m , k , and λ .

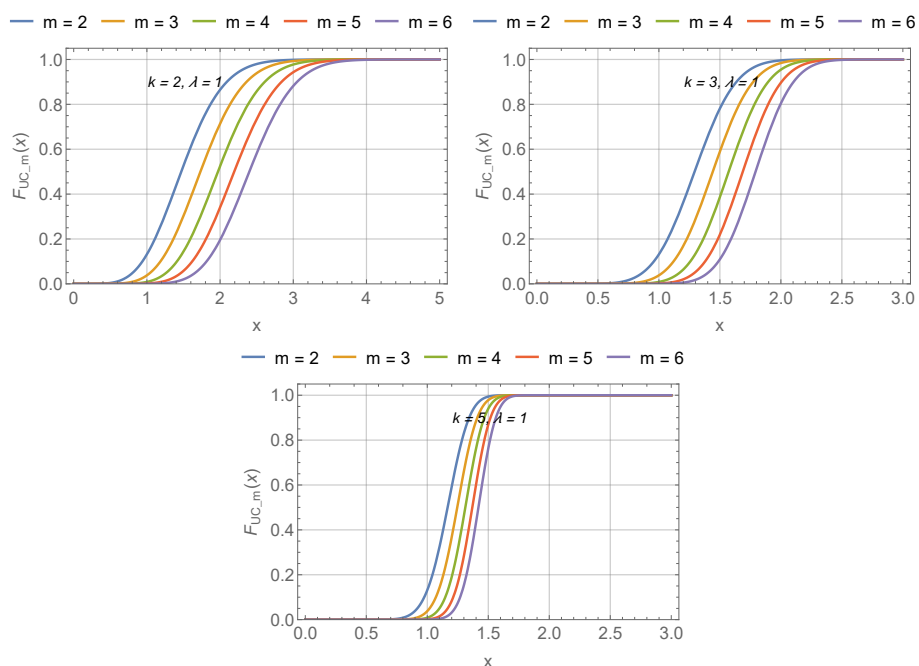


Figure 4. Plot of $F_{UC_m}(x)$ for different values of m , k , and λ .

Lemma 1. Let LC_1, LC_2, \dots, LC_m be the first m lower current record, then the joint pdf of LC_s and LC_m for $1 < m < s$ can be given by

$$f_{LC_m, LC_s}(l_m, l_s) = \frac{f(l_m)f(l_s)}{F(l_m)(s-m-1)!} \left(H(l_m) - H(l_s) \right)^{s-m-1}, \quad l_s < l_m, \quad (2.11)$$

where $H(x) = \ln F(x)$. Now, the conditional probability of LC_s given $LC_m = x_m$ can be written as

$$f_{LC_s|LC_m}(l_s | l_m) = \frac{f(l_s)}{F(l_m)(s-m-1)!} (H(l_m) - H(l_s))^{s-m-1}, \quad l_s < l_m. \quad (2.12)$$

Lemma 2. Let UC_1, UC_2, \dots, UC_m be the first m upper current record, then the joint pdf of UC_s and UC_m for $1 < m < s$ can be given by

$$f_{UC_m, UC_s}(u_m, u_s) = \frac{f(u_m)f(u_s)}{(1-F(u_m))(s-m-1)!} (R(u_s) - R(u_m))^{s-m-1}, \quad u_s > u_m, \quad (2.13)$$

where $R(x) = -\ln(1-F(x))$. Now, the conditional probability of UC_s given $UC_m = u_m$ can be written as

$$f_{UC_s|UC_m}(u_s | u_m) = \frac{f(u_s)}{(1-F(u_m))(s-m-1)!} (R(u_s) - R(u_m))^{s-m-1}, \quad u_s > u_m. \quad (2.14)$$

For proof of Lemmas 1 and 2, one can see [15].

3. Moments of Weibull current records

Moments are among the most useful statistical measures, providing insights into the central tendency, variability, and shape of a distribution. In this section, we derive expressions for the r -th moment of the lower and upper current records for the Weibull distribution.

Theorem 2. Let X follow a Weibull distribution with shape parameter $k > 0$ and scale parameter $\lambda > 0$, and let LC_m and UC_m denote the m -th lower and upper current records, respectively. Then the r -th moments of LC_m and UC_m are given by:

$$E[(LC_m)^r] = 2^m \lambda^r \left[\Gamma\left(1 + \frac{r}{k}\right) - \sum_{p=0}^{\infty} a_p \left(\frac{r}{k}\right) \frac{1 - \left(\frac{r}{k} + p + 2\right)^{-m}}{\frac{r}{k} + p + 1} \right], \quad (3.1)$$

$$E[(UC_m)^r] = 2^m \lambda^r \Gamma(1 + r/k) \left[1 - \left(\frac{2}{3}\right)^{1+r/k} \sum_{q=0}^{m-1} \frac{\Gamma(1 + r/k + q)}{\Gamma(1 + r/k) q!} \left(\frac{1}{3}\right)^q \right], \quad (3.2)$$

where $a_p \left(\frac{r}{k}\right)$ are the coefficients from the expansion:

$$[-\ln(1-t)]^{r/k} = \sum_{p=0}^{\infty} a_p(r/k) t^{r/k+p}, \quad |t| < 1. \quad (3.3)$$

Proof. By definition, the r -th moment of the lower and upper current records is

$$E[(LC_m)^r] = \int_0^{\infty} x^r f_{LC_m}(x; k, \lambda) dx, \quad E[(UC_m)^r] = \int_0^{\infty} x^r f_{UC_m}(x; k, \lambda) dx.$$

Substituting $f_{LC_m}(x; k, \lambda)$ and $f_{UC_m}(x; k, \lambda)$ from Theorem 1 and using the transformation $t = (x/\lambda)^k$, $x = \lambda t^{1/k}$, and $dx = \frac{\lambda}{k} t^{1/k-1} dt$, we obtain

$$E[(LC_m)^r] = 2^m \lambda^r \int_0^\infty t^{r/k} e^{-t} P(m, -\log(1 - e^{-t})) dt,$$

and similarly,

$$E[(UC_m)^r] = 2^m \lambda^r \int_0^\infty t^{r/k} e^{-t} P(m, \frac{t}{2}) dt.$$

These integrals can be evaluated by the following steps:

(1) Expectation of $(LC_m)^r$: Let $y = 1 - e^{-t}$, which gives

$$E[(LC_m)^r] = 2^m \lambda^r \int_0^1 [-\ln(1 - y)]^{r/k} P(m, -\ln y) dy.$$

For integer m ,

$$P(m, u) = 1 - e^{-u} \sum_{j=0}^{m-1} \frac{u^j}{j!}$$

with $u = -\ln y$, substituting this into the integral and splitting it gives

$$E[(LC_m)^r] = 2^m \lambda^r \int_0^1 [-\ln(1 - y)]^{r/k} dy - 2^m \lambda^r \sum_{j=0}^{m-1} \frac{1}{j!} \int_0^1 y(-\ln y)^j [-\ln(1 - y)]^{r/k} dy.$$

Define

$$J_j = \int_0^1 y(-\ln y)^j [-\ln(1 - y)]^{r/k} dy.$$

The first integral is simple:

$$\int_0^1 [-\ln(1 - y)]^{r/k} dy = \Gamma\left(1 + \frac{r}{k}\right).$$

Thus,

$$E[(LC_m)^r] = 2^m \lambda^r \left\{ \Gamma\left(1 + \frac{r}{k}\right) - \sum_{j=0}^{m-1} \frac{1}{j!} J_j \right\}.$$

Now, expanding J_j using the power series expansion (13) and substituting it into the definition of J_j ,

$$J_j = \sum_{p=0}^{\infty} a_p \left(\frac{r}{k}\right) \int_0^1 y^{r/k+p+1} (-\ln y)^j dy.$$

Using the standard identity

$$\int_0^1 x^\alpha (-\ln x)^j dx = \frac{\Gamma(j+1)}{(\alpha+1)^{j+1}} = \frac{j!}{(\alpha+1)^{j+1}},$$

with $\alpha = \frac{r}{k} + p + 1$, we obtain

$$J_j = j! \sum_{p=0}^{\infty} a_p \left(\frac{r}{k}\right) \left(\frac{r}{k} + p + 2\right)^{-(j+1)}.$$

Substituting into the last integral moment, we reach

$$E[(LC_m)^r] = 2^m \lambda^r \left[\Gamma\left(1 + \frac{r}{k}\right) - \sum_{j=0}^{m-1} \sum_{p=0}^{\infty} a_p \left(\frac{r}{k}\right) \left(\frac{r}{k} + p + 2\right)^{-(j+1)} \right].$$

The finite inner sum can be evaluated as

$$\sum_{j=0}^{m-1} \left(\frac{r}{k} + p + 2\right)^{-(j+1)} = \frac{1 - \left(\frac{r}{k} + p + 2\right)^{-m}}{\frac{r}{k} + p + 1}.$$

Hence, we get (11).

(2) Expectation of $(UC_m)^r$: Substituting $P(m, y) = 1 - e^{-y} \sum_{q=0}^{m-1} \frac{y^q}{q!}$ with $y = t/2$ gives

$$E[(UC_m)^r] = 2^m \lambda^r \left\{ \int_0^{\infty} t^{k/\lambda} e^{-t} dt - \sum_{q=0}^{m-1} \frac{1}{q!} \int_0^{\infty} t^{k/\lambda} e^{-t} e^{-t/2} \left(\frac{t}{2}\right)^q dt \right\}.$$

Evaluate the integrals directly:

$$\int_0^{\infty} t^{k/\lambda} e^{-t} dt = \Gamma(1 + k/\lambda), \quad \int_0^{\infty} t^{k/\lambda+q} e^{-(3/2)t} dt = \frac{\Gamma(1 + k/\lambda + q)}{(3/2)^{1+k/\lambda+q}}.$$

Substituting with the last results gives (12). □

4. Parameter estimation

For practical applications, the shape parameter k and the scale parameter λ are typically unknown and must be estimated. Two common approaches are maximum likelihood estimation (MLE) and Bayesian estimation, both of which can be applied to current record data.

4.1. Maximum likelihood estimation (MLE)

Let UC_1, UC_2, \dots, UC_m denote the first n upper current record values from this sequence. The joint PDF of the record values is defined by Barakat et. al. [12] to be

$$f_{UC_1, UC_2, \dots, UC_m}(x_1, x_2, \dots, x_m) = \frac{\bar{F}^2(x_m; k, \lambda) F(x_1; k, \lambda)}{\bar{F}(x_1; k, \lambda)} \left(\prod_{j=1}^m \frac{2f(x_j; k, \lambda)}{\bar{F}(x_j; k, \lambda)} \right), \quad x_1 < x_2 < \dots < x_m, \quad (4.1)$$

and for the $L_1^C, L_2^C, \dots, L_n^m$ as the n lower current record, it was defined as

$$f_{LC_1, LC_2, \dots, LC_m}(x_1, x_2, \dots, x_m) = \frac{\bar{F}^2(x_m; k, \lambda) \bar{F}(x_1; k, \lambda)}{F(x_1; k, \lambda)} \left(\prod_{j=1}^m \frac{2f(x_j; k, \lambda)}{F(x_j; k, \lambda)} \right), \quad x_1 > x_2 > \dots > x_m. \quad (4.2)$$

For current records, the likelihood is proportional to this joint distribution, since it depends only on the current record sequence. Given a set of observed upper current record values UC_1, UC_2, \dots, UC_m with original data follows the Weibull distribution, and the likelihood function based on Eq (15) will be

$$L(k, \lambda|UC) = 2^m k^m \lambda^{-mk} \left(e^{(x_1/\lambda)^k} - 1 \right) e^{-2(x_m/\lambda)^k} \prod_{j=1}^m x_j^{k-1}. \quad (4.3)$$

The log-likelihood is

$$\ell(k, \lambda|UC) = m(\ln 2 + \ln k - k \ln \lambda) + \ln(e^{(x_1/\lambda)^k} - 1) - 2\left(\frac{x_m}{\lambda}\right)^k + (k-1) \sum_{j=1}^m \ln x_j.$$

Differentiating with respect to k and λ and setting it to zero, we get

$$-\frac{mk}{\lambda} - \frac{kx_1^k e^{(x_1/\lambda)^k}}{\lambda^{k+1} (e^{(x_1/\lambda)^k} - 1)} + \frac{2kx_m^k}{\lambda^{k+1}} = 0, \quad (4.4)$$

$$\frac{m}{k} - m \ln \lambda + \frac{(x_1/\lambda)^k e^{(x_1/\lambda)^k} \ln(x_1/\lambda)}{e^{(x_1/\lambda)^k} - 1} - 2\left(\frac{x_m}{\lambda}\right)^k \ln(x_m/\lambda) + \sum_{j=1}^m \ln x_j = 0. \quad (4.5)$$

Solving the resulting nonlinear equations yields the MLEs \hat{k}_{UC}^{ML} from (18) and $\hat{\lambda}_{UC}^{ML}$ from (19), which can be computed numerically using Newton–Raphson or Fisher scoring methods.

The Newton–Raphson method is an iterative optimization algorithm used to find maximum likelihood estimates by solving the score equations. Given a log-likelihood function $\ell(\theta)$, the method updates parameter estimates using $\theta^{(t+1)} = \theta^{(t)} - \mathbf{H}^{-1}(\theta^{(t)})\mathbf{U}(\theta^{(t)})$, where $\mathbf{U}(\theta)$ is the score vector and $\mathbf{H}(\theta)$ is the Hessian matrix of second derivatives. Regarding Hessian definiteness: In finite samples, the observed Hessian is not guaranteed to be positive definite, especially far from the optimum or with poorly behaved likelihood surfaces. Only at the true maximum (with regular conditions) should the Hessian be negative definite, corresponding to a local maximum. For Newton–Raphson to work properly in practice, adjustments like modifying eigenvalues or switching to Fisher scoring (which uses the expected Fisher information matrix, typically positive definite) are often employed when the Hessian fails to be invertible or loses appropriate definiteness during iterations.

An analogous work can be done for the lower current record values LC_1, LC_2, \dots, LC_m with original data, and the Weibull distribution, where the likelihood function based on (16) can be

$$L(k, \lambda|LC) = \frac{2^m k^m e^{-2(x_m/\lambda)^k} e^{-(x_1/\lambda)^k}}{\lambda^m (1 - e^{-(x_1/\lambda)^k})} \prod_{j=1}^m \frac{\left(\frac{x_j}{\lambda}\right)^{k-1} e^{-(x_j/\lambda)^k}}{(1 - e^{-(x_j/\lambda)^k})}. \quad (4.6)$$

Taking the log will turn it into

$$\begin{aligned} \ell(k, \lambda|LC) = & m \ln 2 + m \ln k - m \ln \lambda + (k-1) \sum_{j=1}^m \ln x_j - 2\left(\frac{x_1}{\lambda}\right)^k - \sum_{j=2}^m \left(\frac{x_j}{\lambda}\right)^k \\ & - \ln(1 - e^{-(x_1/\lambda)^k}) - \sum_{j=2}^m \ln(1 - e^{-(x_j/\lambda)^k}), \end{aligned}$$

with respect to k and λ , finding the differentiation and equating it to zero, we bring

$$\frac{m}{k} + \sum_{j=1}^m \ln x_j - 2 \left(\frac{x_1}{\lambda}\right)^k \ln \frac{x_1}{\lambda} - \sum_{j=2}^m \left(\frac{x_j}{\lambda}\right)^k \ln \frac{x_j}{\lambda} - \frac{\left(\frac{x_1}{\lambda}\right)^k \ln \frac{x_1}{\lambda}}{e^{(x_1/\lambda)^k} - 1} - \sum_{j=2}^m \frac{\left(\frac{x_j}{\lambda}\right)^k \ln \frac{x_j}{\lambda}}{e^{(x_j/\lambda)^k} - 1} = 0, \quad (4.7)$$

$$-\frac{m}{\lambda} + \frac{k}{\lambda} \left[2 \left(\frac{x_1}{\lambda}\right)^k + \sum_{j=2}^m \left(\frac{x_j}{\lambda}\right)^k + \frac{\left(\frac{x_1}{\lambda}\right)^k}{e^{(x_1/\lambda)^k} - 1} + \sum_{j=2}^m \frac{\left(\frac{x_j}{\lambda}\right)^k}{e^{(x_j/\lambda)^k} - 1} \right] = 0, \quad (4.8)$$

where (21) is used to find the estimation of \hat{k}_{LC}^{ML} and (22) is used to find it for $\hat{\lambda}_{LC}^{ML}$.

4.2. Bayesian estimate (BE)

Bayesian estimation is important because it incorporates prior knowledge together with observed data to produce more flexible and informative parameter estimates. Unlike classical methods that rely solely on sample information, the Bayesian framework updates beliefs through the posterior distribution, enabling uncertainty to be quantified directly. This leads to more robust inference in situations with limited data, complex models, or when expert knowledge is available. As a result, Bayesian estimation provides a coherent and powerful approach for decision-making, prediction, and uncertainty assessment across a wide range of scientific and applied fields. For more readings about BE, see [10, 14, 16].

4.2.1. BE for upper current records

For BE of the upper current record distribution's estimators, we assume independent priors:

$$\pi(k) \propto k^{a_1-1} e^{-b_1 k}, \quad \pi(\lambda) \propto \lambda^{a_2-1} e^{-b_2 \lambda},$$

and by using the likelihood function given by (20), the joint posterior is then proportional to

$$\pi(k, \lambda | \underline{UC}) \propto k^{m+a_1-1} \lambda^{-mk+a_2-1} \left(e^{(x_1/\lambda)^k} - 1 \right) e^{-2(x_m/\lambda)^k - b_1 k - b_2 \lambda} \prod_{j=1}^m x_j^{k-1}. \quad (4.9)$$

The BE of parameter k symbolized by \hat{k}_{UC}^{BE} under the Square Error Loss (SEL) function is the mean of the posterior density of k given the set of upper current records \underline{UC} , which will be given by

$$E(k | \underline{UC}) = \int_0^\infty \int_0^\infty k \pi(k, \lambda | \underline{UC}) dk d\lambda, \quad (4.10)$$

while $\hat{\lambda}_{UC}^{BE}$, which is the BE of λ under the same set \underline{UC} , can be calculated from

$$E(\lambda | \underline{UC}) = \int_0^\infty \int_0^\infty \lambda \pi(k, \lambda | \underline{UC}) dk d\lambda. \quad (4.11)$$

4.2.2. BE for lower current records

The following priors will be assumed to find the BE of the lower current record distribution's estimator

$$\pi(k) \propto k^{c_1-1} e^{-d_1 k}, \quad \pi(\lambda) \propto \lambda^{c_2-1} e^{-d_2 \lambda}.$$

Now, using the likelihood function represented in (23), we get the following posterior proportional function

$$\pi(k, \lambda | \underline{LC}) \propto k^{m+c_1-1} \lambda^{-m+c_2-1} \frac{1}{1 - e^{-(x_1/\lambda)^k}} e^{-2(x_m/\lambda)^k - (x_1/\lambda)^k - \sum_{j=1}^m (x_j/\lambda)^k - d_1 k - d_2 \lambda} \prod_{j=1}^m \frac{(x_j/\lambda)^{k-1}}{1 - e^{-(x_j/\lambda)^k}}. \quad (4.12)$$

To find the BE of the parameters k and λ symbolized by \hat{k}_{LC}^{BE} and $\hat{\lambda}_{LC}^{BE}$ under SEL function and the set of lower current records \underline{LC} , the following integrals can be used

$$E(k | \underline{LC}) = \int_0^\infty \int_0^\infty k \pi(k, \lambda | \underline{LC}) dk d\lambda, \quad (4.13)$$

$$E(\lambda | \underline{LC}) = \int_0^\infty \int_0^\infty \lambda \pi(k, \lambda | \underline{LC}) dk d\lambda. \quad (4.14)$$

Finding a closed form for (27), (28), (30), and (31) is very hard because of the complex forms (26) and (29) that exist in them. This means we must use one of the numerical methods that can help find these integrals, such as the Markov Chain Monte Carlo (MCMC) method, along with its common algorithm, the Metropolis–Hastings (MH) algorithm, to obtain these estimates.

5. Prediction of future current record values

By incorporating specialized prediction intervals tailored to the current record type and leveraging refined estimators, researchers can obtain more precise and informative forecasts, leading to stronger statistical inference and more robust predictive modeling.

5.1. Non Bayesian prediction intervals (Non-BPI)

Predicting future lower or upper current records, as well as future record ranges, had not been explored before the work of Barakat et al. [12], who established prediction intervals for these quantities. These intervals depend on the most recent observed current record and a computed term that varies depending on the type of current record under consideration (lower, upper, or range). Within these intervals appears a quantity denoted by $Q_{s,\alpha}$, where s indicates the position of the future current record to be predicted. Specifically, $s = 1$ corresponds to the first predicted value, $s = 2$ to the second, and so on, up to a maximum of five predicted values, while α represents the significance level. Values of $Q_{s,\alpha}$ have been tabulated in the literature.

In our approach, we adjust the interval construction procedure by estimating k and λ based on the interval type. If the interval concerns upper current records, we use \hat{k}_{UC}^{ML} or \hat{k}_{UC}^{BE} instead of the original estimator \hat{k} computed from the entire dataset and $\hat{\lambda}_{UC}^{ML}$ or $\hat{\lambda}_{UC}^{BE}$ instead of the original estimator $\hat{\lambda}$. Conversely, for intervals involving lower current records, we employ \hat{k}_{LC}^{ML} or \hat{k}_{LC}^{BE} and $\hat{\lambda}_{LC}^{ML}$ or $\hat{\lambda}_{LC}^{BE}$. This modification leads to more accurate predictive intervals.

The following algorithm outlines the steps for the prediction procedure:

- Step 1.* For any given dataset, determine the distribution F that best fits the observations.
- Step 2.* Extract the observed lower and upper current record values and compute the corresponding record range values. Let m denote the number of observed lower and upper current records.
- Step 3.* Estimate \hat{k}_{LC}^{ML} and $\hat{\lambda}_{LC}^{ML}$ or \hat{k}_{LC}^{BE} and $\hat{\lambda}_{LC}^{BE}$ using the methods mentioned in Subsection 4.1 and 4.2. Also, estimate \hat{k}_{UC}^{ML} and $\hat{\lambda}_{UC}^{ML}$ or \hat{k}_{UC}^{BE} and $\hat{\lambda}_{UC}^{BE}$.
- Step 4.* Determine the position s of the future current record to be predicted and the desired significance level α . Then obtain the value of $Q_{s,\alpha}$ from the tables provided by Barakat et al. [12].
- Step 5.* Using the estimates from step 3, determine the lower and upper bounds of the predictive confidence intervals as follows:

- 1) $(UC_m, F^{-1}(1 - \bar{F}^{1+Q_{s,\alpha}}(UC_m)))$ is a $(1 - \alpha)\%$ confidence interval for UC_{m+s} .
- 2) $(F^{-1}(F^{1+Q_{s,\alpha}}(LC_m)), LC_m)$ is a $(1 - \alpha)\%$ confidence interval for LC_{m+s} .
- 3) $(UC_m - LC_m, F^{-1}(1 - \bar{F}^{1+Q_{s,\alpha}}(UC_m)) - F^{-1}(F^{1+Q_{s,\alpha}}(LC_m)))$ is a $\beta\%$ confidence interval for RC_{m+s} , where $\beta \geq \max(1 - 2\alpha, 0)$.

5.2. Bayesian prediction (BP) and Bayesian predictive interval (BPI)

BP is a statistical approach that uses Bayes' theorem to make predictions by combining prior beliefs about unknown parameters with information from observed data. Instead of producing a single point estimate, it accounts for uncertainty by integrating over the posterior distribution of the parameters. This results in a predictive distribution for future observations, which naturally reflects data variability and parameter uncertainty. From this predictive distribution, BPIs can be derived, providing a range of plausible values for future observations along with a specified probability of coverage. As more data become available, the predictions and their associated predictive intervals are updated coherently and consistently, making BP especially useful in situations with limited data or when prior knowledge is important.

5.2.1. BP and BPI for upper current records

Let UC_s denote the next upper current record value following the observed upper current record sequence. The predictive density of f_{UC_s} given \underline{UC} is

$$f_{UC_s|\underline{UC}}^p(u_s|k, \lambda) = \int_0^\infty \int_0^\infty f_{UC_s|UC_m}(u_s|u_m)\pi(k, \lambda|\underline{UC}) d\lambda dk, \quad (5.1)$$

where $f_{UC_s|UC_m}(u_s|u_m)$ is given by (14). By substituting by (1) and (2) in (14) and multiplying the result by (26), we get

$$f_{UC_s|\underline{UC}}^p(u_s|k, \lambda) = \int_0^\infty \int_0^\infty k^{m+a_1} \lambda^{-mk+a_2-k-1} \left(\frac{u_s}{\lambda}\right)^{k-1} \left[\left(\frac{u_s}{\lambda}\right)^k - \left(\frac{u_m}{\lambda}\right)^k \right]^{s-m-1} (e^{(u_1/\lambda)^k} - 1) \exp\left\{-\left(\frac{u_s}{\lambda}\right)^k - \left(\frac{u_m}{\lambda}\right)^k - b_1k - b_2\lambda\right\} \times \prod_{j=1}^m u_j^{k-1} d\lambda dk. \quad (5.2)$$

Now, under the squared-error loss function, the Bayesian point predictor of the future upper current record UC_s is the posterior predictive mean, given by

$$\widehat{UC}_s^{\text{BP}} = E(UC_s | \underline{UC}) = \int_{u_m}^{\infty} u_s f_{UC_s|\underline{UC}}^p(u_s) du_s. \quad (5.3)$$

Due to the analytical intractability of the predictive density in (33), the expectation in (34) does not admit a closed-form expression. Consequently, the Bayesian point predictor is approximated using the posterior predictive simulation as

$$\widehat{UC}_s^{\text{BP}} \approx \frac{1}{T} \sum_{t=1}^T UC_s^{(t)},$$

where $\{UC_s^{(t)}\}_{t=1}^T$ are realizations from the posterior predictive distribution.

For the Bayesian Predictive Interval, a $100(1 - \alpha)\%$ Bayesian predictive interval for UC_s is defined as

$$P(L_\alpha \leq UC_s \leq U_\alpha | \underline{UC}) = 1 - \alpha,$$

where the lower and upper bounds satisfy

$$\int_{u_m}^{L_\alpha} f_{UC_s|\underline{UC}}^p(u_s) du_s = \frac{\alpha}{2}, \quad (5.4)$$

$$\int_{u_m}^{U_\alpha} f_{UC_s|\underline{UC}}^p(u_s) du_s = 1 - \frac{\alpha}{2}. \quad (5.5)$$

In practice, the predictive interval is obtained from the empirical quantiles of the posterior predictive sample $\{UC_s^{(t)}\}_{t=1}^T$ as

$$(L_\alpha, U_\alpha) = (Q_{\alpha/2}, Q_{1-\alpha/2}),$$

where Q_p denotes the p th quantile of the posterior predictive distribution.

5.2.2. BP and BPI for lower current records

For lower current records, the prediction of future values proceeds in a manner analogous to the upper record case, though with important differences reflecting the decreasing nature of lower records. Let LC_s represent the s th lower current record to be predicted ($s > m$, where m is the number of observed records). The posterior predictive density for LC_s conditional on the observed sequence $\underline{LC} = (LC_1, LC_2, \dots, LC_m)$ is

$$f_{LC_s|\underline{LC}}^p(l_s|k, \lambda) = \int_0^\infty \int_0^\infty f_{LC_s|LC_m}(l_s|l_m), \pi(k, \lambda|\underline{LC}), d\lambda, dk, \quad (5.6)$$

where $f_{LC_s|LC_m}(l_s|l_m)$ follows from (12). Combining the conditional density from (12) with the posterior distribution in (29) yields the explicit form

$$f_{LC_s|\underline{LC}}^p(l_s|k, \lambda) = \int_0^\infty \int_0^\infty k^{m+c_1} \lambda^{-m+c_2-k-1} \left(\frac{l_s}{\lambda}\right)^{k-1} \left[-\ln(1 - e^{-(l_m/\lambda)^k}) + \ln(1 - e^{-(l_s/\lambda)^k})\right]^{s-m-1} \\ \times \frac{1}{1 - e^{-(l_1/\lambda)^k}} \exp\left\{-2\left(\frac{l_m}{\lambda}\right)^k - \left(\frac{l_1}{\lambda}\right)^k - \sum_{j=1}^m \left(\frac{l_j}{\lambda}\right)^k - d_1 k - d_2 \lambda\right\} \prod_{j=1}^m \frac{(l_j/\lambda)^{k-1}}{1 - e^{-(l_j/\lambda)^k}} d\lambda dk. \quad (5.7)$$

The Bayesian point predictor under squared-error loss is the mean of this predictive distribution:

$$\widehat{LC}_s^{\text{BP}} = E(LC_s | \underline{LC}) = \int_0^{l_m} l_s f_{LC_s|\underline{LC}}^p(l_s) dl_s. \quad (5.8)$$

As with the upper record case, analytical evaluation of (39) is not feasible. Hence, Monte Carlo approximation is employed:

$$\widehat{LC}_s^{\text{BP}} \approx \frac{1}{T} \sum_{t=1}^T LC_s^{(t)},$$

where $\{LC_s^{(t)}\}_{t=1}^T$ drawn from the posterior predictive distribution via MCMC sampling.

A $100(1 - \gamma)\%$ Bayesian predictive interval (L_γ, U_γ) for LC_s satisfies

$$P(L_\gamma \leq LC_s \leq U_\gamma | \underline{LC}) = 1 - \gamma,$$

with endpoints determined by

$$\int_0^{L_\gamma} f_{LC_s|\underline{LC}}^p(l_s) dl_s = \gamma/2, \quad \int_0^{U_\gamma} f_{LC_s|\underline{LC}}^p(l_s) dl_s = 1 - \gamma/2. \quad (5.9)$$

These limits are approximated from the ordered posterior predictive sample $\{LC_s^{(t)}\}_{t=1}^T$ as

$$(L_\gamma, U_\gamma) = (q_{\gamma/2}, q_{1-\gamma/2}),$$

where $LC_s^{(t)}$ denotes the t th ordered value.

Note that, unlike upper records, lower current records are decreasing: $LC_s < LC_m$ for $s > m$. Consequently, any credible interval for LC_s is bounded above by l_m , the most recent observed lower record. This constraint must be respected in the simulation and the interpretation of predictive intervals.

6. Numerical illustration

6.1. Simulation study

In this section, we present simulation results and estimation procedures for the Weibull current record data. Since the Weibull distribution is widely used in reliability analysis, survival studies, and wind speed modeling, the ability to accurately estimate its parameters from current records is of significant practical importance.

To simulate lower and upper current records when the parent population follows the Weibull distribution, the following algorithm is applied:

- a. Generate a random sample X_1, X_2, \dots, X_m from a Weibull distribution with known parameters (k, λ) using the inverse transform method:

$$X_i = \lambda [-\log(1 - U_i)]^{1/k}, \quad U_i \sim U(0, 1).$$

- b. Initialize:

$$LC_1 = X_1, \quad UC_1 = X_1.$$

- c. For $i > 1$, when the i th record (of either kind) is detected from the sequence $\{X_i\}$, update the current records as follows:

- If the new observation is a new lower record, then

$$LC_i = X_i, \quad UC_i = UC_{i-1}.$$

- If the new observation is a new upper record, then

$$UC_i = X_i, \quad LC_i = LC_{i-1}.$$

- If none, do nothing and move to the next $\{X_i\}$.

Repeat the process 1000 times with samples of size 100 and then compute the mean of the estimates for each current sample size m , together with the corresponding standard deviation (SD). The number of sample size m appears among the 1000 samples represented by n . In addition, the root mean square error (RMSE) and the mean absolute deviation (MAD) are evaluated to assess the accuracy of the estimates. Additionally, bootstrap confidence intervals (BCIs) are calculated for each parameter. All these results are summarized in Tables 1–3. As using MCMC, along with the MH algorithm, requires initial values for the parameters, we use the estimates from the MLE as those.

Table 1. Results of the simulation when $k = 2$ and $\lambda = 1$.

m	Parameter	MLE			BE		
		Mean \pm SD	RMSE/MAD	95% BCI	Mean \pm SD	RMSE/MAD	95% BCI
4 (n=17)	k_{UC}	5.1961 \pm 3.5653	4.3231 / 3.8075	[1.0829, 7.4028]	3.1531 \pm 1.9791	1.9852 / 1.8022	[1.0265, 4.9410]
	λ_{UC}	1.5729 \pm 0.5774	0.7419 / 0.6302	[0.9140, 1.9908]	1.3811 \pm 0.4991	0.5580 / 0.4853	[0.8438, 1.8303]
	k_{LC}	0.4771 \pm 0.0361	1.5233 / 1.5229	[0.4276, 0.5281]	0.4757 \pm 0.0955	1.5271 / 1.5243	[0.2823, 0.5671]
	λ_{LC}	0.4327 \pm 0.3049	0.6398 / 0.5673	[0.0054, 0.8530]	0.4382 \pm 0.3090	0.6367 / 0.5618	[0.0053, 0.8607]
5 (n=23)	k_{UC}	2.3176 \pm 1.6223	1.5907 / 1.2460	[0.7657, 5.3663]	2.1035 \pm 1.4813	1.4269 / 1.1561	[0.3636, 5.8036]
	λ_{UC}	1.1376 \pm 0.4560	0.4592 / 0.3703	[0.4790, 1.7761]	1.0775 \pm 0.4738	0.4618 / 0.3934	[0.1301, 1.7854]
	k_{LC}	0.4770 \pm 0.0367	1.5234 / 1.5230	[0.4389, 0.5465]	0.4438 \pm 0.0962	1.5591 / 1.5562	[0.2745, 0.5892]
	λ_{LC}	0.2247 \pm 0.1943	0.7983 / 0.7753	[0.0057, 0.5842]	0.2274 \pm 0.1980	0.7965 / 0.7726	[0.0055, 0.5943]
6 (n=77)	k_{UC}	2.1884 \pm 1.9955	1.9914 / 1.2007	[0.5486, 7.1536]	2.0035 \pm 1.5530	1.5428 / 1.0589	[0.6056, 6.4242]
	λ_{UC}	0.9952 \pm 0.4497	0.4468 / 0.3666	[0.2378, 2.0555]	0.9727 \pm 0.3989	0.3973 / 0.3240	[0.3748, 1.8333]
	k_{LC}	0.4951 \pm 0.0314	1.5053 / 1.5049	[0.4468, 0.5675]	0.4756 \pm 0.0755	1.5263 / 1.5244	[0.3052, 0.5884]
	λ_{LC}	0.2415 \pm 0.1476	0.7725 / 0.7585	[0.0189, 0.5123]	0.2440 \pm 0.1510	0.7707 / 0.7560	[0.0183, 0.5183]
7 (n=117)	k_{UC}	1.9564 \pm 1.3916	1.3862 / 0.9393	[0.6314, 5.5059]	1.8535 \pm 1.1920	1.1958 / 0.8670	[0.4859, 5.2427]
	λ_{UC}	0.9035 \pm 0.3715	0.3822 / 0.3213	[0.2658, 1.7568]	0.8864 \pm 0.3495	0.3661 / 0.2982	[0.1753, 1.5784]
	k_{LC}	0.5024 \pm 0.0309	1.4979 / 1.4976	[0.4527, 0.5664]	0.4793 \pm 0.0733	1.5225 / 1.5207	[0.3253, 0.6073]
	λ_{LC}	0.2280 \pm 0.1348	0.7835 / 0.7720	[0.0313, 0.5568]	0.2300 \pm 0.1381	0.7822 / 0.7700	[0.0307, 0.5686]
8 (n=143)	k_{UC}	3.1735 \pm 8.9881	9.0330 / 1.8954	[0.8488, 9.2972]	3.0768 \pm 8.9018	8.9355 / 1.8113	[0.8668, 8.5185]
	λ_{UC}	0.9793 \pm 0.3791	0.3783 / 0.3104	[0.3728, 1.8071]	0.9672 \pm 0.3503	0.3506 / 0.2892	[0.3858, 1.6509]
	k_{LC}	0.5175 \pm 0.0293	1.4827 / 1.4825	[0.4659, 0.5782]	0.5075 \pm 0.0666	1.4940 / 1.4925	[0.3539, 0.6145]
	λ_{LC}	0.2574 \pm 0.1217	0.7524 / 0.7426	[0.0519, 0.5281]	0.2599 \pm 0.1249	0.7505 / 0.7401	[0.0508, 0.5402]
9 (n=175)	k_{UC}	2.3397 \pm 2.0209	2.0436 / 1.0248	[0.8590, 8.6719]	2.3738 \pm 2.0658	2.0936 / 1.0716	[0.8300, 8.1742]
	λ_{UC}	0.9317 \pm 0.3565	0.3620 / 0.2934	[0.3462, 1.7144]	0.9284 \pm 0.3530	0.3592 / 0.2928	[0.3392, 1.7231]
	k_{LC}	0.5208 \pm 0.0319	1.4795 / 1.4792	[0.4677, 0.5883]	0.5055 \pm 0.0695	1.4961 / 1.4945	[0.3790, 0.6289]
	λ_{LC}	0.2441 \pm 0.1156	0.7646 / 0.7559	[0.0764, 0.4825]	0.2462 \pm 0.1191	0.7631 / 0.7538	[0.0757, 0.4958]
10 (n=122)	k_{UC}	2.5497 \pm 6.0544	6.0545 / 1.2276	[0.9304, 4.4296]	2.5133 \pm 6.0245	6.0217 / 1.2415	[0.8833, 4.8897]
	λ_{UC}	0.8564 \pm 0.3086	0.3392 / 0.2847	[0.3466, 1.4725]	0.8375 \pm 0.3061	0.3454 / 0.2885	[0.3566, 1.4906]
	k_{LC}	0.5207 \pm 0.0287	1.4796 / 1.4793	[0.4695, 0.5748]	0.5023 \pm 0.0662	1.4991 / 1.4977	[0.3665, 0.6175]
	λ_{LC}	0.2288 \pm 0.0944	0.7769 / 0.7712	[0.0759, 0.4119]	0.2306 \pm 0.0982	0.7756 / 0.7694	[0.0739, 0.4213]
11 (n=151)	k_{UC}	2.1622 \pm 1.2054	1.2123 / 0.7830	[0.9033, 5.3062]	2.1600 \pm 1.3564	1.3614 / 0.8087	[0.8804, 5.6086]
	λ_{UC}	0.8505 \pm 0.3077	0.3412 / 0.2799	[0.2875, 1.4325]	0.8307 \pm 0.3111	0.3533 / 0.2887	[0.3310, 1.4472]
	k_{LC}	0.5243 \pm 0.0275	1.4759 / 1.4757	[0.4742, 0.5865]	0.5075 \pm 0.0672	1.4940 / 1.4925	[0.3914, 0.6280]
	λ_{LC}	0.2351 \pm 0.0932	0.7705 / 0.7649	[0.0785, 0.4546]	0.2370 \pm 0.0969	0.7691 / 0.7630	[0.0761, 0.4662]
12 (n=68)	k_{UC}	2.1236 \pm 0.9894	0.9897 / 0.6887	[0.9786, 5.1175]	2.0355 \pm 0.8448	0.8393 / 0.6415	[0.9267, 3.8536]
	λ_{UC}	0.8058 \pm 0.2744	0.3345 / 0.2805	[0.3459, 1.2999]	0.7734 \pm 0.2541	0.3390 / 0.2773	[0.3025, 1.2290]
	k_{LC}	0.5312 \pm 0.0227	1.4690 / 1.4688	[0.4861, 0.5793]	0.5220 \pm 0.0580	1.4791 / 1.4780	[0.3883, 0.6390]
	λ_{LC}	0.2510 \pm 0.0844	0.7537 / 0.7490	[0.0689, 0.4302]	0.2538 \pm 0.0889	0.7514 / 0.7462	[0.0658, 0.4505]
13 (n=65)	k_{UC}	2.3471 \pm 1.5897	1.6147 / 0.8485	[1.0879, 6.6855]	2.2850 \pm 1.5626	1.5761 / 0.8341	[0.9556, 7.3602]
	λ_{UC}	0.8265 \pm 0.2935	0.3390 / 0.2916	[0.3919, 1.7077]	0.7981 \pm 0.2946	0.3552 / 0.2990	[0.3132, 1.7218]
	k_{LC}	0.5270 \pm 0.0274	1.4733 / 1.4730	[0.4896, 0.5879]	0.5102 \pm 0.0709	1.4915 / 1.4898	[0.4091, 0.6449]
	λ_{LC}	0.2368 \pm 0.0944	0.7690 / 0.7632	[0.0999, 0.4544]	0.2390 \pm 0.0994	0.7674 / 0.7610	[0.0964, 0.4680]
14 (n=20)	k_{UC}	1.9228 \pm 0.7695	0.7540 / 0.5892	[1.0381, 3.8772]	1.9222 \pm 0.7721	0.7565 / 0.5855	[1.1000, 4.1185]
	λ_{UC}	0.7115 \pm 0.2512	0.3784 / 0.3464	[0.3636, 1.3052]	0.7045 \pm 0.2442	0.3794 / 0.3474	[0.4159, 1.3387]
	k_{LC}	0.5339 \pm 0.0350	1.4665 / 1.4661	[0.4864, 0.5983]	0.5158 \pm 0.0790	1.4862 / 1.4842	[0.3758, 0.6726]
	λ_{LC}	0.2362 \pm 0.0948	0.7693 / 0.7638	[0.0979, 0.4408]	0.2377 \pm 0.1003	0.7685 / 0.7623	[0.0929, 0.4549]
15 (n=12)	k_{UC}	2.1308 \pm 0.9169	0.8875 / 0.6700	[1.0505, 4.1740]	2.0017 \pm 0.7509	0.7189 / 0.6067	[0.9187, 3.4447]
	λ_{UC}	0.7746 \pm 0.2744	0.3462 / 0.3076	[0.3748, 1.3356]	0.7306 \pm 0.2522	0.3618 / 0.2976	[0.3056, 1.1691]
	k_{LC}	0.5237 \pm 0.0227	1.4765 / 1.4763	[0.4906, 0.5822]	0.5000 \pm 0.0521	1.5009 / 1.5000	[0.4191, 0.6122]
	λ_{LC}	0.2217 \pm 0.0619	0.7806 / 0.7783	[0.1373, 0.3111]	0.2219 \pm 0.0657	0.7807 / 0.7781	[0.1340, 0.3190]
16 (n=10)	k_{UC}	2.4092 \pm 0.5959	0.6357 / 0.4765	[1.8990, 3.0641]	2.5268 \pm 0.5212	0.6772 / 0.5268	[2.0767, 3.0979]
	λ_{UC}	0.7920 \pm 0.1625	0.2467 / 0.2080	[0.6528, 0.9706]	0.8192 \pm 0.1264	0.2081 / 0.1808	[0.7153, 0.9599]
	k_{LC}	0.5309 \pm 0.0184	1.4692 / 1.4691	[0.5098, 0.5436]	0.5031 \pm 0.0418	1.4973 / 1.4969	[0.4557, 0.5345]
	λ_{LC}	0.2218 \pm 0.0380	0.7788 / 0.7782	[0.1939, 0.2651]	0.2206 \pm 0.0417	0.7801 / 0.7794	[0.1875, 0.2674]

Table 2. Results of the simulation when $k = 3$ and $\lambda = 1$.

m	Parameter	MLE			BE		
		Mean \pm SD	RMSE/MAD	95% BCI	Mean \pm SD	RMSE/MAD	95% BCI
4 (n=14)	k_{UC}	4.2202 \pm 2.1447	2.2735 / 1.8208	[1.5172, 6.5962]	3.5954 \pm 1.6344	1.5784 / 1.3493	[1.4688, 5.4722]
	λ_{UC}	1.2994 \pm 0.2650	0.3819 / 0.3583	[0.8527, 1.5314]	1.2181 \pm 0.2335	0.3020 / 0.2864	[0.8292, 1.4388]
	k_{LC}	0.4617 \pm 0.0217	2.5384 / 2.5383	[0.4278, 0.4911]	0.4588 \pm 0.0581	2.5418 / 2.5412	[0.3557, 0.5088]
	λ_{LC}	0.3017 \pm 0.1739	0.7175 / 0.6983	[0.0529, 0.4797]	0.3047 \pm 0.1762	0.7151 / 0.6953	[0.0527, 0.4867]
5 (n=32)	k_{UC}	2.7471 \pm 1.3639	1.3589 / 1.0976	[0.9563, 5.6389]	2.6312 \pm 1.4568	1.4731 / 1.3004	[0.9235, 5.7073]
	λ_{UC}	1.0277 \pm 0.2267	0.2237 / 0.1985	[0.5595, 1.3424]	0.9593 \pm 0.2741	0.2714 / 0.2258	[0.5073, 1.3612]
	k_{LC}	0.4711 \pm 0.0226	2.5290 / 2.5289	[0.4405, 0.5224]	0.4655 \pm 0.0513	2.5350 / 2.5345	[0.3778, 0.5561]
	λ_{LC}	0.2752 \pm 0.1339	0.7367 / 0.7248	[0.0793, 0.5723]	0.2776 \pm 0.1356	0.7346 / 0.7224	[0.0789, 0.5778]
6 (n=63)	k_{UC}	3.7169 \pm 5.8590	5.8540 / 2.2114	[0.9156, 14.9927]	3.7806 \pm 5.9545	5.9560 / 2.2276	[0.7897, 17.2036]
	λ_{UC}	0.9841 \pm 0.2884	0.2864 / 0.2379	[0.4702, 1.4858]	0.9733 \pm 0.2977	0.2964 / 0.2341	[0.3900, 1.5505]
	k_{LC}	0.4777 \pm 0.0215	2.5224 / 2.5223	[0.4468, 0.5135]	0.4691 \pm 0.0536	2.5315 / 2.5309	[0.3552, 0.5550]
	λ_{LC}	0.2638 \pm 0.1142	0.7449 / 0.7362	[0.0580, 0.4874]	0.2656 \pm 0.1167	0.7434 / 0.7344	[0.0569, 0.4918]
7 (n=118)	k_{UC}	3.9728 \pm 6.7112	6.7527 / 2.4163	[1.0799, 19.8558]	3.9707 \pm 6.6941	6.7355 / 2.4580	[1.0225, 17.9891]
	λ_{UC}	0.9540 \pm 0.3109	0.3130 / 0.2644	[0.4281, 1.5800]	0.9303 \pm 0.3035	0.3101 / 0.2586	[0.4253, 1.5817]
	k_{LC}	0.4888 \pm 0.0211	2.5113 / 2.5112	[0.4527, 0.5322]	0.4819 \pm 0.0492	2.5186 / 2.5181	[0.3813, 0.5613]
	λ_{LC}	0.2606 \pm 0.0993	0.7459 / 0.7394	[0.0871, 0.4373]	0.2628 \pm 0.1011	0.7441 / 0.7372	[0.0869, 0.4416]
8 (n=153)	k_{UC}	3.3778 \pm 2.8364	2.8522 / 1.5969	[1.1687, 13.2582]	3.2545 \pm 2.5793	2.5834 / 1.5391	[1.1777, 11.3739]
	λ_{UC}	0.9407 \pm 0.2656	0.2713 / 0.2270	[0.4319, 1.4418]	0.9105 \pm 0.2564	0.2707 / 0.2265	[0.4797, 1.4765]
	k_{LC}	0.4948 \pm 0.0220	2.5053 / 2.5052	[0.4590, 0.5467]	0.4877 \pm 0.0505	2.5128 / 2.5123	[0.3785, 0.5716]
	λ_{LC}	0.2578 \pm 0.0853	0.7470 / 0.7422	[0.0940, 0.4071]	0.2600 \pm 0.0877	0.7452 / 0.7400	[0.0926, 0.4157]
9 (n=160)	k_{UC}	3.3412 \pm 2.7101	2.7230 / 1.3761	[1.3003, 6.6968]	3.3477 \pm 2.8967	2.9083 / 1.4296	[1.2448, 8.2777]
	λ_{UC}	0.9431 \pm 0.2407	0.2465 / 0.2031	[0.4628, 1.4015]	0.9192 \pm 0.2483	0.2603 / 0.2148	[0.4526, 1.3966]
	k_{LC}	0.5022 \pm 0.0234	2.4979 / 2.4978	[0.4671, 0.5550]	0.4961 \pm 0.0504	2.5044 / 2.5039	[0.3952, 0.5854]
	λ_{LC}	0.2620 \pm 0.0812	0.7424 / 0.7380	[0.0947, 0.3912]	0.2643 \pm 0.0841	0.7404 / 0.7357	[0.0928, 0.4028]
10 (n=150)	k_{UC}	3.6244 \pm 4.2098	4.2418 / 1.4528	[1.5229, 8.4970]	3.5488 \pm 4.1327	4.1552 / 1.4229	[1.4918, 9.6051]
	λ_{UC}	0.9326 \pm 0.2047	0.2149 / 0.1753	[0.5422, 1.4144]	0.8969 \pm 0.2108	0.2340 / 0.1904	[0.5404, 1.4136]
	k_{LC}	0.5038 \pm 0.0186	2.4963 / 2.4962	[0.4715, 0.5430]	0.5004 \pm 0.0416	2.5000 / 2.4996	[0.4058, 0.5717]
	λ_{LC}	0.2657 \pm 0.0647	0.7371 / 0.7343	[0.1225, 0.3838]	0.2683 \pm 0.0673	0.7348 / 0.7317	[0.1202, 0.3942]
11 (n=142)	k_{UC}	3.2837 \pm 1.7679	1.7844 / 1.0635	[1.5694, 8.8183]	3.1671 \pm 1.6220	1.6249 / 1.0132	[1.4547, 8.2765]
	λ_{UC}	0.9007 \pm 0.1997	0.2224 / 0.1798	[0.5163, 1.3095]	0.8639 \pm 0.2002	0.2415 / 0.2001	[0.4986, 1.2859]
	k_{LC}	0.5068 \pm 0.0174	2.4933 / 2.4932	[0.4804, 0.5476]	0.5008 \pm 0.0437	2.4996 / 2.4992	[0.4076, 0.5820]
	λ_{LC}	0.2595 \pm 0.0649	0.7434 / 0.7405	[0.1288, 0.3797]	0.2618 \pm 0.0681	0.7414 / 0.7382	[0.1264, 0.3852]
12 (n=81)	k_{UC}	3.1239 \pm 1.8274	1.8198 / 1.0598	[1.5129, 10.8460]	3.0432 \pm 1.7906	1.7796 / 1.0953	[1.4832, 7.4793]
	λ_{UC}	0.8522 \pm 0.2069	0.2532 / 0.2070	[0.4556, 1.4168]	0.8153 \pm 0.2074	0.2767 / 0.2373	[0.4840, 1.3869]
	k_{LC}	0.5087 \pm 0.0177	2.4913 / 2.4913	[0.4832, 0.5451]	0.5027 \pm 0.0379	2.4976 / 2.4973	[0.4447, 0.5737]
	λ_{LC}	0.2579 \pm 0.0561	0.7442 / 0.7421	[0.1636, 0.3561]	0.2603 \pm 0.0590	0.7420 / 0.7397	[0.1607, 0.3667]
13 (n=50)	k_{UC}	3.2090 \pm 1.3939	1.3938 / 1.0584	[1.6576, 6.6606]	3.1211 \pm 1.5571	1.5440 / 1.1153	[1.6142, 6.7516]
	λ_{UC}	0.8377 \pm 0.1846	0.2442 / 0.1963	[0.5542, 1.4136]	0.7974 \pm 0.1970	0.2810 / 0.2399	[0.4925, 1.1724]
	k_{LC}	0.5131 \pm 0.0152	2.4870 / 2.4869	[0.4863, 0.5465]	0.5078 \pm 0.0377	2.4925 / 2.4922	[0.4459, 0.5700]
	λ_{LC}	0.2621 \pm 0.0534	0.7398 / 0.7379	[0.1763, 0.3381]	0.2645 \pm 0.0564	0.7377 / 0.7355	[0.1740, 0.3462]
14 (n=13)	k_{UC}	2.6421 \pm 1.0217	1.0449 / 0.8581	[1.5524, 5.5213]	2.5453 \pm 0.9327	1.0049 / 0.9295	[1.5540, 4.5379]
	λ_{UC}	0.7632 \pm 0.1695	0.2874 / 0.2583	[0.5081, 1.1318]	0.7258 \pm 0.1731	0.3207 / 0.2798	[0.4966, 1.0370]
	k_{LC}	0.5127 \pm 0.0151	2.4873 / 2.4873	[0.4946, 0.5402]	0.5003 \pm 0.0450	2.5000 / 2.4997	[0.4255, 0.5916]
	λ_{LC}	0.2392 \pm 0.0576	0.7628 / 0.7608	[0.1434, 0.3678]	0.2414 \pm 0.0626	0.7609 / 0.7586	[0.1400, 0.3861]
15 (n=15)	k_{UC}	3.0516 \pm 1.3492	1.3045 / 1.0845	[1.5142, 5.6118]	3.0140 \pm 1.4810	1.4308 / 1.1545	[1.3522, 6.1216]
	λ_{UC}	0.7672 \pm 0.2194	0.3149 / 0.2649	[0.4246, 1.1342]	0.7358 \pm 0.2380	0.3502 / 0.3027	[0.3677, 1.1688]
	k_{LC}	0.5007 \pm 0.0123	2.4993 / 2.4993	[0.4782, 0.5168]	0.4780 \pm 0.0449	2.5224 / 2.5220	[0.3913, 0.5405]
	λ_{LC}	0.2418 \pm 0.0576	0.7603 / 0.7582	[0.1423, 0.3300]	0.2419 \pm 0.0613	0.7604 / 0.7581	[0.1359, 0.3345]
16 (n=9)	k_{UC}	2.6247 \pm 0.8019	0.8095 / 0.6235	[1.4422, 3.6207]	2.5115 \pm 0.9097	0.9490 / 0.7807	[1.1722, 3.7304]
	λ_{UC}	0.7388 \pm 0.2097	0.3216 / 0.2612	[0.4256, 1.0000]	0.6860 \pm 0.2530	0.3870 / 0.3157	[0.2964, 1.0043]
	k_{LC}	0.5100 \pm 0.0136	2.4900 / 2.4900	[0.4928, 0.5309]	0.4916 \pm 0.0344	2.5086 / 2.5084	[0.4385, 0.5348]
	λ_{LC}	0.2353 \pm 0.0571	0.7664 / 0.7647	[0.1400, 0.2887]	0.2372 \pm 0.0590	0.7646 / 0.7628	[0.1393, 0.2933]

Table 3. Results of the simulation when $k = 5$ and $\lambda = 1$.

m	Parameter	MLE			BE		
		Mean \pm SD	RMSE/MAD	95% BCI	Mean \pm SD	RMSE/MAD	95% BCI
4 (n=14)	k_{UC}	4.6667 \pm 5.5228	5.2500 / 3.6348	[0.0347, 9.0603]	4.0421 \pm 4.7917	4.6457 / 3.8006	[0.0517, 8.0976]
	λ_{UC}	0.8276 \pm 0.7793	0.7003 / 0.726	[0.0543, 1.7276]	0.73799 \pm 0.7337	0.7337 / 0.3799	[0.0049, 1.4899]
	k_{LC}	0.4404 \pm 0.0108	4.5596 / 4.5596	[0.4276, 0.4566]	0.4344 \pm 0.0353	4.5657 / 4.5656	[0.3841, 0.4774]
	λ_{LC}	0.2717 \pm 0.1150	0.7365 / 0.7283	[0.1105, 0.4347]	0.2735 \pm 0.1162	0.7349 / 0.7265	[0.1111, 0.4361]
5 (n=16)	k_{UC}	5.7703 \pm 7.6888	7.4491 / 3.8419	[1.7785, 10.250]	5.8490 \pm 7.0959	6.8902 / 3.4110	[1.6521, 10.645]
	λ_{UC}	0.9798 \pm 0.1687	0.1638 / 0.1388	[0.7251, 1.2823]	1.0014 \pm 0.1875	0.1807 / 0.1571	[0.6895, 1.2724]
	k_{LC}	0.4528 \pm 0.0101	4.5472 / 4.5472	[0.4397, 0.4736]	0.4502 \pm 0.0263	4.5499 / 4.5498	[0.4062, 0.4918]
	λ_{LC}	0.2882 \pm 0.0739	0.7154 / 0.7118	[0.2009, 0.4360]	0.2906 \pm 0.0759	0.7132 / 0.7094	[0.2010, 0.4412]
6 (n=73)	k_{UC}	7.2942 \pm 6.9162	7.2391 / 4.1009	[1.4519, 9.4649]	7.0636 \pm 7.0128	7.2612 / 4.1130	[1.5823, 10.879]
	λ_{UC}	1.0331 \pm 0.1781	0.1799 / 0.1523	[0.6098, 1.2936]	1.0013 \pm 0.1907	0.1893 / 0.1645	[0.6252, 1.2957]
	k_{LC}	0.4701 \pm 0.0111	4.5299 / 4.5299	[0.4468, 0.4877]	0.4739 \pm 0.0271	4.5262 / 4.5261	[0.3874, 0.5107]
	λ_{LC}	0.3066 \pm 0.0642	0.6963 / 0.6934	[0.1341, 0.3965]	0.3097 \pm 0.0654	0.6934 / 0.6903	[0.1342, 0.3994]
7 (n=107)	k_{UC}	6.1890 \pm 6.4614	6.5393 / 3.3862	[1.7066, 9.7929]	5.9017 \pm 6.2557	6.2905 / 3.3892	[1.7077, 9.0564]
	λ_{UC}	0.9677 \pm 0.1811	0.1831 / 0.1476	[0.6035, 1.2711]	0.9312 \pm 0.1929	0.2039 / 0.1708	[0.5736, 1.2841]
	k_{LC}	0.4723 \pm 0.0108	4.5277 / 4.5277	[0.4532, 0.4940]	0.4711 \pm 0.0298	4.5290 / 4.5289	[0.4032, 0.5185]
	λ_{LC}	0.2871 \pm 0.0637	0.7157 / 0.7129	[0.1198, 0.4076]	0.2894 \pm 0.0654	0.7135 / 0.7106	[0.1188, 0.4102]
8 (n=146)	k_{UC}	6.9896 \pm 10.454	10.606 / 3.6238	[2.2290, 8.3324]	7.1256 \pm 10.631	10.804 / 3.9871	[1.9300, 8.4167]
	λ_{UC}	0.9862 \pm 0.1540	0.1541 / 0.1175	[0.6728, 1.2803]	0.9566 \pm 0.1888	0.1931 / 0.1560	[0.5758, 1.2461]
	k_{LC}	0.4799 \pm 0.0113	4.5202 / 4.5201	[0.4601, 0.5023]	0.4800 \pm 0.0298	4.5201 / 4.5200	[0.4177, 0.5247]
	λ_{LC}	0.2913 \pm 0.0597	0.7112 / 0.7087	[0.1628, 0.3978]	0.2938 \pm 0.0615	0.7088 / 0.7062	[0.1629, 0.3987]
9 (n=154)	k_{UC}	6.2416 \pm 5.8078	5.9202 / 2.8779	[2.3267, 7.3063]	6.0226 \pm 5.8574	5.9269 / 2.9007	[2.0479, 7.6112]
	λ_{UC}	0.9642 \pm 0.1443	0.1483 / 0.1226	[0.7233, 1.2473]	0.9293 \pm 0.1666	0.1805 / 0.1498	[0.6045, 1.2667]
	k_{LC}	0.4822 \pm 0.0109	4.5179 / 4.5178	[0.4616, 0.5025]	0.4802 \pm 0.0303	4.5199 / 4.5198	[0.4201, 0.5325]
	λ_{LC}	0.2848 \pm 0.0538	0.7172 / 0.7152	[0.1759, 0.3743]	0.2876 \pm 0.0559	0.7146 / 0.7124	[0.1769, 0.3823]
10 (n=173)	k_{UC}	5.9473 \pm 4.9497	5.0255 / 2.5413	[2.4549, 7.4585]	5.8576 \pm 5.0037	5.0624 / 2.5596	[2.2722, 7.8859]
	λ_{UC}	0.9408 \pm 0.1393	0.1510 / 0.1223	[0.6708, 1.2288]	0.9172 \pm 0.1590	0.1789 / 0.1415	[0.6313, 1.2373]
	k_{LC}	0.4856 \pm 0.0105	4.5144 / 4.5144	[0.4687, 0.5075]	0.4838 \pm 0.0262	4.5163 / 4.5162	[0.4363, 0.5324]
	λ_{LC}	0.2845 \pm 0.0441	0.7169 / 0.7155	[0.2038, 0.3660]	0.2871 \pm 0.0461	0.7144 / 0.7129	[0.2031, 0.3702]
11 (n=127)	k_{UC}	5.2134 \pm 2.5830	2.5816 / 1.9041	[2.3167, 7.4141]	5.1451 \pm 2.6609	2.6542 / 1.9707	[2.3191, 7.4567]
	λ_{UC}	0.9151 \pm 0.1401	0.1634 / 0.1331	[0.6167, 1.1722]	0.8894 \pm 0.1573	0.1918 / 0.1582	[0.5832, 1.1781]
	k_{LC}	0.4878 \pm 0.0092	4.5122 / 4.5122	[0.4707, 0.5056]	0.4859 \pm 0.0274	4.5142 / 4.5141	[0.4349, 0.5338]
	λ_{LC}	0.2849 \pm 0.0456	0.7166 / 0.7151	[0.1934, 0.3671]	0.2875 \pm 0.0476	0.7141 / 0.7125	[0.1948, 0.3743]
12 (n=67)	k_{UC}	5.2292 \pm 2.0470	2.0433 / 1.6524	[2.5402, 8.7240]	5.2865 \pm 2.4150	2.4125 / 1.7927	[2.5702, 8.9109]
	λ_{UC}	0.9102 \pm 0.1218	0.1506 / 0.1204	[0.6921, 1.1154]	0.8901 \pm 0.1325	0.1713 / 0.1455	[0.6681, 1.1352]
	k_{LC}	0.4896 \pm 0.0091	4.5104 / 4.5104	[0.4748, 0.5119]	0.4854 \pm 0.0260	4.5147 / 4.5146	[0.4093, 0.5276]
	λ_{LC}	0.2811 \pm 0.0433	0.7201 / 0.7189	[0.1579, 0.3522]	0.2834 \pm 0.0451	0.7180 / 0.7166	[0.1566, 0.3563]
13 (n=62)	k_{UC}	5.2118 \pm 2.3455	2.3321 / 1.6715	[2.4211, 9.479]	4.9237 \pm 2.2374	2.2167 / 1.5340	[2.3653, 9.517]
	λ_{UC}	0.9000 \pm 0.1245	0.1588 / 0.1317	[0.6898, 1.1280]	0.8671 \pm 0.1311	0.1857 / 0.1615	[0.6057, 1.1306]
	k_{LC}	0.4931 \pm 0.0094	4.5069 / 4.5069	[0.4727, 0.5088]	0.4911 \pm 0.0271	4.5089 / 4.5089	[0.4289, 0.5393]
	λ_{LC}	0.2836 \pm 0.0384	0.7174 / 0.7164	[0.2040, 0.3436]	0.2863 \pm 0.0412	0.7149 / 0.7137	[0.1975, 0.3517]
14 (n=36)	k_{UC}	5.2303 \pm 2.2323	2.2103 / 1.6654	[2.8222, 10.237]	5.0575 \pm 2.3812	2.3455 / 1.9312	[2.6142, 10.778]
	λ_{UC}	0.8897 \pm 0.1082	0.1533 / 0.1315	[0.7079, 1.1234]	0.8509 \pm 0.1393	0.2026 / 0.1736	[0.6555, 1.1047]
	k_{LC}	0.4899 \pm 0.0080	4.5101 / 4.5101	[0.4791, 0.5135]	0.4826 \pm 0.0253	4.5175 / 4.5174	[0.4350, 0.5343]
	λ_{LC}	0.2812 \pm 0.0357	0.7196 / 0.7188	[0.2083, 0.3432]	0.2832 \pm 0.0388	0.7178 / 0.7168	[0.2015, 0.3452]
15 (n=17)	k_{UC}	4.7314 \pm 1.7179	1.6849 / 1.2123	[0.0375, 7.2718]	4.8751 \pm 2.4434	2.3691 / 1.6567	[0.0379, 7.815]
	λ_{UC}	0.3461 \pm 0.3044	0.3844 / 0.461	[0.042, 0.7367]	0.2565 \pm 0.1026	0.9026 / 0.2565	[0.1542, 0.3591]
	k_{LC}	0.4937 \pm 0.0090	4.5063 / 4.5063	[0.4824, 0.5170]	0.4942 \pm 0.0211	4.5058 / 4.5058	[0.4635, 0.5426]
	λ_{LC}	0.2961 \pm 0.0254	0.7043 / 0.7039	[0.2362, 0.3355]	0.2995 \pm 0.0282	0.7010 / 0.7005	[0.2343, 0.3415]
16 (n=8)	k_{UC}	4.6190 \pm 1.2854	1.2112 / 0.9505	[2.8246, 6.4238]	4.4942 \pm 1.1476	1.1443 / 0.8267	[2.6481, 5.4690]
	λ_{UC}	0.8370 \pm 0.1232	0.1967 / 0.1630	[0.6367, 0.9713]	0.8110 \pm 0.1284	0.2212 / 0.1890	[0.5948, 0.9084]
	k_{LC}	0.4955 \pm 0.0097	4.5045 / 4.5045	[0.4808, 0.5063]	0.4928 \pm 0.0320	4.5073 / 4.5072	[0.4389, 0.5320]
	λ_{LC}	0.2845 \pm 0.0428	0.7166 / 0.7155	[0.2284, 0.3454]	0.2897 \pm 0.0490	0.7117 / 0.7103	[0.2255, 0.3593]

Overall, the simulation results indicate that parameter estimation based on current record data is feasible, but its accuracy depends strongly on the number of observed current records, the type of

record (upper or lower), and the true value of the Weibull shape parameter k . As the current record size increases, both estimation methods exhibit improved performance, as reflected in lower standard deviations, smaller RMSE/MAD values, and narrower confidence and credible intervals.

For small current record sizes (e.g., sizes 4–6), the estimation of the upper record shape parameter k_{UC} shows substantial variability, particularly under MLE. This is evidenced by large standard deviations and inflated RMSE values, especially when the true shape parameter is moderate to large (e.g., $k = 3$ or $k = 5$). Such behavior is expected due to the limited information content of early upper current records, leading to a relatively flat likelihood surface.

In comparison, the Bayesian predictor yields smaller RMSE/MAD values and more concentrated estimates for small record sizes, indicating superior robustness in sparse-data situations. As the current record size increases, MLE and BE converge toward the true value of k , and the difference between the two methods becomes negligible.

The estimation of scale parameter λ_{UC} is generally more stable than that of k_{UC} . Even for small record sizes, both methods produce estimates close to the true value $\lambda = 1$, with relatively low RMSE and MAD. The BE again shows slightly reduced variability and narrower credible intervals for small and moderate record sizes. For larger record sizes, the performance of MLE and BE becomes nearly identical.

In contrast to the upper record case, the estimates of the lower record shape parameter k_{LC} are highly stable across all record sizes and values of k . The estimated means exhibit minimal fluctuation, and the associated standard deviations remain small.

However, the RMSE and MAD values remain relatively large and nearly constant across current record sizes. This phenomenon reflects the inherent limitation of lower current records, which provide little information about the upper tail of the Weibull distribution. Consequently, increasing the number of lower current records does not substantially improve the estimation accuracy of k_{LC} . MLE and BE show similar behavior in this regard.

The estimate of the lower record scale parameter λ_{LC} shows moderate variability for small current record sizes but gradually stabilizes as the number of records increases. The RMSE and MAD values decrease slowly, and interval estimates become narrower. The BE offers marginal improvements in small samples, while both methods perform comparably for larger record sizes.

A comparison of Tables 1–3 reveals that larger true values of the Weibull shape parameter k lead to increased estimation difficulty, particularly for the upper current record shape parameter k_{UC} . For $k = 5$, MLE and BE exhibit larger standard deviations and RMSE values, even for moderate record sizes. This behavior is consistent with the Weibull distribution's increased tail sensitivity as k increases.

Despite this challenge, the Bayesian predictor maintains relatively better stability than MLE in small-sample scenarios.

The reported BCI of MLE and BE generally includes the true parameter values, especially for moderate and large current record sizes. For small sizes, the intervals, particularly for k_{UC} , are wide, reflecting substantial uncertainty inherent in record-based inference.

Bayesian BCIs are often slightly narrower and more centered around the true parameter values in small samples, further supporting the advantage of BP when information is limited.

In summary, the simulation study demonstrates that:

- Upper current records are more informative than lower current records for estimating Weibull parameters, particularly the shape parameter, and this, of course, because of the way the lower

current records are formulated.

- The BE outperforms MLE for small current record sizes, offering lower variability and improved accuracy.
- As the number of current records increases, both methods converge and exhibit comparable performance.
- Larger values of the Weibull shape parameter k increase estimation difficulty, highlighting the practical benefits of Bayesian methods in such settings.

These findings support the use of BE techniques for Weibull current record data, especially in reliability and survival analysis applications where only a limited number of records are available.

6.2. Saudi Arabian industry data: Real example

In Saudi Arabia, the water supply, sewerage, waste management, and remediation activities sector plays a growing role within the Industrial Production Index (IPI), reflecting the Kingdom's strategic focus on environmental sustainability and infrastructure development. This sector captures the performance of desalination plants, water distribution networks, wastewater treatment facilities, solid waste management, and environmental remediation services, all of which are critical in a water-scarce economy. Trends in the IPI for this activity are closely linked to government investment under Vision 2030, population growth, urban expansion, and industrial demand for reliable water and sanitation services. Rising index values generally indicate increased operational capacity, efficiency improvements, and expanded coverage of water and waste service. Fluctuations, on the other hand, may reflect seasonal demand, maintenance cycles, or changes in public expenditure. As environmental regulations tighten and private sector participation increases, this sector's contribution to the IPI is expected to become more stable and increasingly significant in assessing Saudi Arabia's industrial and environmental performance. The dataset consists of the IPI, expressed as an index number relative to a base year set equal to 100, which measures changes in industrial output over time rather than physical production units. The following data are the monthly index for the water supply, sewerage, waste management, and remediation activities from January 2023 to August 2025 of size 32 obtained from the Saudi General Authority of Statistics (SGAS):

109.2, 107.6, 113.0, 118.6, 118.1, 120.0, 121.6, 125.3, 116.2, 111.4, 104.1, 112.1, 108.9, 107.7, 109.9, 115.3, 120.8, 122.0, 122.9, 124.2, 119.1, 120.7, 115.1, 112.9, 122.8, 121.8, 126.4, 122.8, 126.9, 129.9, 130.9, 131.6.

This can be found among other IPI data on this link: <https://www.stats.gov.sa/en/statistics-tabs?tab=436312&category=123454>. After trying to find a fit distribution to these data, we find that the best fitted distribution is the Weibull distribution $W(k, \lambda)$ with estimated shape parameter $\hat{k} = 18.3881$ and an estimated scale parameter $\hat{\lambda} = 121.787$. The goodness-of-fit tests used to ensure this are the Kolmogorov-Smirnov test (p-value = 0.93978), the Anderson-Darling test (p-value = 0.928562), and the Cramér-von Mises test (p-value = 0.945796). Figure 5 shows the estimated Weibull PDF and CDF against the given data.

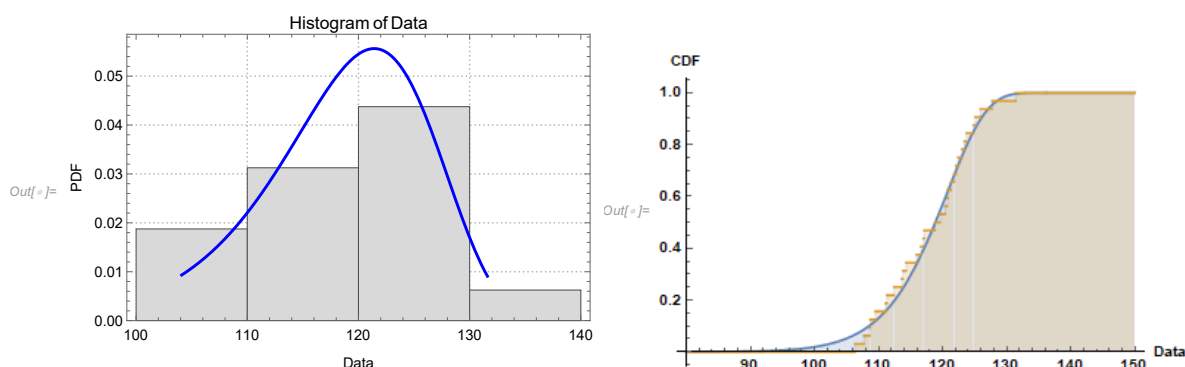


Figure 5. $W(18.3881, 121.787)$'s PDF and CDF against the real data.

Now, to predict the future upper and lower currents and the record range, we use the proposed two techniques: Non-BPI and BP with BPI.

1) Non-BPI:

To do this, we apply the proposed algorithm in Subsection 5.1 as follows:

- A. As mentioned, the data does fit the Weibull distribution with $\hat{k} = 18.3881$ and $\hat{\lambda} = 121.787$.
B.

Table 4. Values of LC_m , UC_m , and RC_m from the data.

m	1	2	3	4	5	6	7	8	9	10	11	12	13
UC_m	109.2	109.2	113	118.6	120	121.6	125.3	125.3	126.4	126.9	129.9	130.9	131.6
LC_m	109.2	107.6	107.6	107.6	107.6	107.6	107.6	104.1	104.1	104.1	104.1	104.1	104.1
RC_m	0	1.6	5.4	11	12.4	14	17.7	21.2	22.3	22.8	25.8	26.8	27.5

- C. As the simulation study in Subsection (6.1) indicates that the BE outperforms the MLE, we use it to estimate our parameters. Using equations from Subsection (4.2), we find that $\hat{k}_{UC}^{BE} = 5.04763$ with 95% credible intervals (CI) (2.58586, 8.58294), $\hat{\lambda}_{UC}^{BE} = 84.7555$ with CI (54.5819, 106.779), $\hat{k}_{LC}^{BE} = 11.9629$ with CI (6.42938, 19.3019), and $\hat{\lambda}_{LC}^{Be} = 109.75$ with CI (104.298, 117.894).

- D. To predict the next three upper and lower currents, it means that when $s = 1, 2,$ and $3,$ the values of $Q_{s,\alpha}$ at $\alpha = 0.05$ and $m = 13$ will be $Q_{1,0.05} = 0.223828,$ $Q_{2,0.05} = 0.364064,$ and $Q_{3,0.05} = 0.492298.$ The Non-BPI for the future three current records are shown in Table 5.

E.

Table 5. Non-BPI for the next three current records.

$m = 13$	UC_{m+s}	LC_{m+s}	RC_{m+s}
$s = 1$	(131.600, 136.973)	(101.920, 104.100)	(27.500, 35.052)
$s = 2$	(131.600, 139.949)	(100.639, 104.100)	(27.500, 39.310)
$s = 3$	(131.600, 142.462)	(99.511, 104.100)	(27.500, 42.951)

2) BP with BPI:

To predict future upper current records using BP with BPI, we apply equations (34)–(36) to the

data given in Table 4. Analogous work can be obtained to lower current records using equations (39) and (40). We make predictions for the next three current records, along with their BPIs for $s = 1, 2$, and 3 , and show the results in Table 6.

Table 6. BP and BPI for the next three current records.

$m = 13$	$\hat{U}C_{m+s}$	$\hat{L}C_{m+s}$	$\hat{R}C_{m+s}$
$s = 1$	132.024(131.613, 133.016)	103.901(103.715, 104.087)	28.123(27.898, 28.929)
$s = 2$	133.147(131.820, 134.863)	103.754(103.343, 104.081)	29.393(28.477, 30.782)
$s = 3$	134.560(132.395, 136.635)	103.572(102.998, 104.072)	30.988(29.397, 32.563)

The Non-BPI method provides only interval estimates and yields relatively wide prediction ranges that expand rapidly as the forecast horizon increases, reflecting higher uncertainty and conservative bounds. In contrast, the BP with BPI approach produces point predictions and predictive intervals that are substantially narrower and evolve more smoothly over time. While Non-BPI fixes one bound at the last observed record and enables the opposite bound to vary widely, BP with BPI centers the intervals around gradually changing point estimates. Overall, BP with BPI delivers more precise and stable forecasts than Non-BPI across all future horizons.

7. Conclusions

In this paper, we developed a comprehensive statistical framework for modeling, estimating, and predicting current record values from a two-parameter Weibull distribution, a widely used model for reliability, survival analysis, and industrial applications. We derived explicit probability density and cumulative distribution functions for lower and upper current records, along with general expressions for their moments. These theoretical results provide the foundation for inference when only record-breaking observations, rather than the full sample, are available.

From an inferential perspective, we presented and compared two principal estimation approaches: Maximum likelihood estimation and Bayesian estimation. The simulation study demonstrated that Bayesian methods offer superior performance in small-record scenarios, yielding more stable estimates with reduced variability and narrower credible intervals. As the number of observed records increases, both estimation methods converge, though Bayesian estimation remains advantageous when prior information is available or when the Weibull shape parameter is large.

A major contribution of this work is the development of practical prediction procedures for future current records. We adapted classical non-Bayesian prediction intervals by incorporating record-specific parameter estimates, leading to more accurate uncertainty bounds. Furthermore, we introduced a fully Bayesian predictive framework that naturally accounts for parameter uncertainty through the posterior predictive distribution, providing point predictions and associated Bayesian predictive intervals.

The methodology was applied to real-world data from Saudi Arabia's water supply, sewerage, waste management, and remediation sectors, illustrating its utility for monitoring industrial performance indicators. The Weibull distribution provided an excellent fit to the index data, and the proposed prediction methods generated plausible forecasts for future upper and lower records, with Bayesian prediction yielding more precise and interpretable intervals than the classical approach.

In summary, this study provides a comprehensive toolkit for analyzing Weibull-distributed current record data, bridging theoretical derivations, estimation methods, and predictive applications. The results support the use of Bayesian methods, especially when record sequences are short or when prior knowledge is relevant. In future studies, researchers could extend the framework to other lifetime distributions, incorporate co-variates, or explore multivariate record processes, further enhancing the applicability of record-based inference in industrial, environmental, and reliability contexts.

Use of Generative-AI tools declaration

The author declares he has not used Artificial Intelligence (AI) tools in the creation of this article.

Acknowledgments

The author extends his appreciation to Prince Sattam bin Abdulaziz University for funding this research work through the project number (PSAU/2025/01/36482).

Conflict of interest

The author confirms there is no conflict of interest.

References

1. J. Ahmadi, N. Balakrishnan, Confidence intervals for quantiles in terms of record range, *Stat. Probabil. Lett.*, **68** (2004), 395–405. <https://doi.org/10.1016/j.spl.2004.04.013>
2. J. Ahmadi, N. Balakrishnan, Distribution-free confidence intervals for quantile intervals based on current records, *Stat. Probabil. Lett.*, **75** (2005), 190–202. <https://doi.org/10.1016/j.spl.2005.05.011>
3. J. Ahmadi, N. Balakrishnan, Preservation of some reliability properties by certain record statistics, *Statistics*, **39** (2005), 347–354. <https://doi.org/10.1080/02331880500178752>
4. J. Ahmadi, M. Razmkhah, N. Balakrishnan, Current k-records and their use in distribution-free confidence intervals, *Stat. Probabil. Lett.*, **79** (2009), 29–37. <https://doi.org/10.1016/j.spl.2008.07.014>
5. J. Ahmadi, N. Balakrishnan, Outer and inner prediction intervals for order statistics intervals based on current records, *Stat. Papers*, **53** (2012), 789–802. <http://doi.org/10.1007/s00362-011-0383-4>
6. R. A. Aldallal, Best linear unbiased estimation and prediction of record values based on Kumaraswamy distributed data, *Statistics, Optimization and Information Computing*, **10** (2022), 1250–1266. <https://doi.org/10.19139/soic-2310-5070-1397>
7. R. A. Aldallal, Moment generating function of current records based on generalized exponential distribution with some recurrence relations, *Eur. J. Pure Appl. Math.*, **16** (2023), 97–111. <https://doi.org/10.29020/nybg.ejpam.v16i1.4641>

8. R. A. Aldallal, Current record range of Laplace distributed data with application on Saudi Arabia industrial data, *Journal of Statistics Applications and Probability*, **14** (2025), 723–729. <https://doi.org/10.18576/jsap/140504>
9. R. A. Aldallal, Rayleigh current record distributed data: estimation and prediction with application on Saudi Arabia industrial data, *J. Stat. Theory Appl.*, **25** (2026), 2. <https://doi.org/10.1007/s44199-025-00150-x>
10. N. Alsadat, C. Taniş, L. P. Sapkota, A. Kumar, W. Marzouk, A. M. Gemeay, Inverse unit exponential probability distribution: Classical and Bayesian inference with applications, *AIP Adv.*, **14** (2024), 055108. <https://doi.org/10.1063/5.0210828>
11. H. M. Barakat, E. M. Nigm, R. A. Aldallal, Current records and record range with some applications, *J. Korean Stat. Soc.*, **43** (2014), 263–273. <https://doi.org/10.1016/j.jkss.2013.09.004>
12. H. M. Barakat, E. M. Nigm, R. A. Aldallal, Exact prediction intervals for future current records and record range from any continuous distribution, *SORT*, **38** (2014), 251–270.
13. M. Chahkandi, J. Ahmadi, Prediction intervals for k-records in terms of current records, *J. Stat. Theory Appl.*, **12** (2013), 67–82. <https://doi.org/10.2991/jsta.2013.12.1.6>
14. I. Elbatal, M. I. A. Araibi, S. K. Ocloo, E. M. Almetwally, L. P. Sapkota, A. M. Gemeay, Classical and Bayesian methodology for a new inverse statistical model, *Engineering Reports*, **7** (2025), e70323. <https://doi.org/10.1002/eng2.70323>
15. R. L. Houchens, Record value theory and inference, PhD Thesis, University of California, 1984.
16. A. A. Khalaf, M. A. Khaleel, E. Hussam, G. T. Gellow, A. T. Hammad, A. M. Gemeay, Bayesian and non-Bayesian approaches for estimating the extended exponential distribution: applications to COVID-19 and carbon fibers, *Innovation in Statistics and Probability*, **1** (2025), 60–94. <https://doi.org/10.64389/isp.2025.01236>
17. D. B. Meng, S. P. Zhu, *Multidisciplinary design optimization of complex structures under uncertainty*, Boca Raton: CRC Press, 2024. <https://doi.org/10.1201/9781003464792>
18. D. B. Meng, Y. P. Guo, Y. H. Xu, S. Y. Yang, Y. Q. Guo, L. D. Pan, et al., Saddlepoint approximation method in reliability analysis: A review, *CMES-Comp. Model. Eng.*, **139** (2024), 2329–2359. <https://doi.org/10.32604/cmes.2024.047507>
19. M. Z. Raqab, Bounds on expectations of record range and record increment from distributions with bounded support, *Journal of Inequalities in Pure and Applied Mathematics*, **8** (2007), 1–11.
20. M. Z. Raqab, Distribution-free prediction intervals for the future current record statistics, *Stat. Papers*, **50** (2009), 429–439. <https://doi.org/10.1007/s00362-007-0082-3>
21. M. Z. Raqab, Inequalities for expected current record statistics, *Commun. Stat.-Theor. M.*, **36** (2007), 1367–1380. <https://doi.org/10.1080/03610920601077097>



AIMS Press

©2026 the Author(s), licensee AIMS Press. This is an open access article distributed under the terms of the Creative Commons Attribution License (<https://creativecommons.org/licenses/by/4.0>)